

Modelling the equilibrium and transient responses of global temperature to past and future trace gas concentrations

Ch Tricot and A Berger

Universite Catholique de Louvain, Institut d'Astronomie et de Géophysique G. Lemaître, 2 Chemin du Cyclotron, B-1348 Louvain-la-Neuve, Belgium

Abstract. Recent works with energy balance climate models and oceanic general circulation models have assessed the potential role of the world ocean for climatic changes on a decadal to secular time scale. This scientific challenge is illustrated by estimating the response of the global temperature to changes in trace gas concentration from the pre-industrial epoch to the middle of the next century. A simple energetic formulation is given to estimate the effect on global equilibrium temperature of a fixed instantaneous radiative forcing and of a time-dependent radiative forcing. An atmospheric energy balance model coupled to a box-advection-diffusion ocean model is then used to estimate the past and future global climatic transient response to trace-gas concentration changes. The time-dependent radiative perturbation is estimated from a revised approximate radiative parameterization, and the recent reference set of trace gas scenarios proposed by Wuebbles et al. (1984) are adopted as standard scenarios. Similar computations for the past and future have recently been undertaken by Wigley (1985), but using a purely diffusive ocean and slightly different trace gas scenarios. The skill of the so-called standard experiment is finally assessed by examining the model sensitivity to different parameters such as the equilibrium surface air temperature change for a doubled CO_2 concentration [$\Delta T_{ae}(2 \times \text{CO}_2)$], the heat exchange with the deeper ocean and the trace gas scenarios. For $\Delta T_{ae}(2 \times \text{CO}_2)$ between 1 K and 5 K, the following main results are obtained: (i) for a pre-industrial CO_2 concentration of 270 ppmv, the surface air warming between 1850 and 1980 ranges between 0.4 and 1.4 K (if a pre-industrial CO_2 concentration of 290 ppmv is chosen, the range is between

0.3 and 1 K); (ii) by comparison with the instantaneous equilibrium computations, the deeper ocean inertia induces a delay which amounts to between 6 years [for lower $\Delta T_{ae}(2 \times \text{CO}_2)$] and 23 years [for higher $\Delta T_{ae}(2 \times \text{CO}_2)$] in 1980; (iii) for the standard future CO_2 and other trace gas scenarios of Wuebbles et al., the surface air warming between 1980 and 2050 is calculated to range between 0.9 and 3.4 K, with a delay amounting to between 7 years and 32 years in 2050 when compared to equilibrium computations.

Introduction

A growing number of theoretical calculations assess the changes in radiative fluxes and in temperature corresponding to a change in trace gas concentrations in the atmosphere, essentially a doubling of the carbon dioxide (CO_2) only or of equivalent CO_2 (UNEP-WMO-ICSU, 1985). A large variety of climatic models have been used to deal with this potentially important climatic question.

Climate models can be classified as either thermodynamic or hydrodynamic models [see the general reviews on climate modelling by Schneider and Dickinson (1974), Gates (1981), Shine and Henderson-Sellers (1983)]. In thermodynamic models [energy balance (EBM) and radiative-convective (RCM) models], the temperature is explicitly predicted but the effect of the motion field on the temperature is neglected or included only in a highly simplified way. The primary goal of thermodynamic climate models is to combine parameterizations of different dominant mechanisms thought to be important for determining the climate. All the feedbacks between these mechanisms can thus be examined in detail,

which allows an increased understanding of the model response.

The most well-known hydrodynamic climate models are the three-dimensional general circulation models (3-D GCMs) which undertake, numerically, the time integration of the primitive equations that describe the detailed evolution of the dynamic and thermodynamic state of the atmosphere and possibly of the ocean. Despite their present limitations, GCMs try to answer many quantitative questions that cannot be resolved with the other models because of the assumptions made in these models. Issues concerning the trace gas problem, such as the time of year the warming is at a maximum, its geographical distribution, the variations of precipitation, snow cover, soil moisture, cloudiness and temperature, can (or could) only be studied in sufficient detail with high-resolution GCMs that include interactive atmospheric and oceanic feedbacks.

Within the framework of the trace gas climate problem, two general types of studies have been performed with such climate models: examining either the climate response in a state of climatic equilibrium to a fixed or to a time-dependent radiative forcing, or the transient climate response to a fixed or to a time-dependent radiative forcing. In an equilibrium study (Gilchrist 1983; Schlesinger 1984), a mathematical model of the climate is perturbed and allowed to reach a new equilibrium. The model time-dependent behaviour is deduced by the numerical approach to the final equilibrium. Such experiments have been conducted, for example, with GCMs including a swamp ocean or a mixed layer (without deeper ocean), for a CO₂ doubling or quadrupling. [It is worth noting that because of the lack of taking the long memory part of the ocean-atmosphere system into account, the equilibrium climate is related only to the atmosphere and possibly to the upper ocean. Moreover, because the characteristic time scale of the forcing (e.g., CO₂ variation) is different from that of the oceanic part of the climate system, the result is probably never in real equilibrium.] If a time-dependent radiative forcing is used, successive equilibrium states are independently reached one after the other ["snapshot" experiments; e.g., Ramanathan et al. (1985), using a global RCM]. These equilibrium studies have highlighted the sensitivity of the model response to the feedback mechanisms included in the models.

The proper inclusion of the heat capacity of thermal reservoirs in the climate system would allow one to assess the transient behaviour of the

climate by comparing the transient climate response at any time with the atmosphere equilibrium response at the same time. The final object of the transient study is therefore to determine the lag in the response of the climate system, the knowledge of which is required to estimate when the trace-gas-induced climate change may become detectable. A few coupled ocean-atmosphere GCMs have recently begun to analyse, for a time period of a few decades, the transient response to an instantaneous CO₂ radiative perturbation (Bryan and Spelman 1985; Schlesinger et al. 1985). Such fixed, instantaneous forcing was used to allow sufficient statistical significance of the simulated climate change over the computed time period. However, the actual trace gas increase is a continuous rise, not an instantaneous step increase, and the actual climate transient behaviour is not straightforwardly deduced from equilibrium simulations or even from transient experiments using a fixed, instantaneous radiative perturbation (Schneider and Thompson 1981). The real detection of the trace gas effects on climate requires a statistically significant signal relative to the background noise of natural temperature fluctuations (e.g., Wigley and Jones 1981). Climatic transient models can help to estimate the time of this detection only if the time-dependent nature of the forcing is taken into account besides the feedback mechanisms and the memory of the climate system.

During the last decade, observational as well as theoretical studies related to the chemistry of the atmosphere have led to the conclusion that there are many other trace gases that have radiative properties similar to CO₂ for which either natural or anthropogenically induced changes can also be of significance. Among them the most important are water vapour, chlorocarbons, nitrous oxide, methane, and ozone in the troposphere and stratosphere (WMO, 1982, 1983 a; Wuebbles et al. 1984; WMO 1986). Recent studies have shown that, although an estimate of their climatic influence is possible (e.g., Ramanathan et al. 1985; Wang et al. 1986), their sources and sinks are not well-known, making estimates of man's impact in this field rather difficult. As a consequence, only a discussion of the climatic impact of an estimated increase (i.e., using scenarios, not predictions) in these trace gases is reasonable.

Finally, aside from the radiative greenhouse effect, the complete trace-gas-induced climate problem involves tropospheric and stratospheric chemistries, chemistry-climate interactions, stratospheric transport and stratosphere/troposphere

radiative-dynamical interactions (WMO 1983 a; WMO 1986). All these chemistry-dynamics climate interactions will not be addressed further in this paper because of numerous uncertainties in the present state of their modelling which would add confusion to the interpretation of climate computations reported here. Thus, for example, ozone changes have not been considered in the present study, although these may well be important (Ramanathan et al. 1985; Wang et al. 1986). Such simplification must be kept in mind when assessing the range of uncertainty related to the computed warming due to changes in trace gas concentrations in the near future.

In this paper, we use globally and annually averaged energy balance considerations to assess the potential climatic importance of trace gases. In the next section, we briefly review the present state-of-the-art of the equilibrium response modelling for a CO₂ increase. We introduce a simple formulation to estimate the effect on global equilibrium temperature for a fixed instantaneous or time-dependent radiative forcing. In the subsequent section, the transient response is calculated by using a simple box-advection-diffusion atmosphere/ocean energy balance model and a time-dependent forcing function to give a range of estimates of the trace-gas-induced climatic changes since the pre-industrial period and in the next decades. Based on our present knowledge of the climatic system behaviour and on estimates of future trace gas concentrations, a potential range of the trace-gas-induced temperature increase is given for the period up to the middle of the next century. The various uncertainties related to the present estimates of future climatic warming are also stressed.

Modelling the equilibrium response

Brief review of present results

Reviews of the equilibrium climate simulations related to a doubling or a quadrupling of atmospheric CO₂ have been given recently by Manabe (1983), Schlesinger (1984), Dickinson (1985) and Schlesinger and Mitchell (1985). We will not duplicate here these excellent general reviews but summarize, in Fig. 1, most of the results obtained with climate models for doubling the CO₂ concentration. Next we will comment on some particular points in such equilibrium computations.

In Fig. 1 we excluded the GCM simulations with a prescribed sea surface temperature (e.g.,

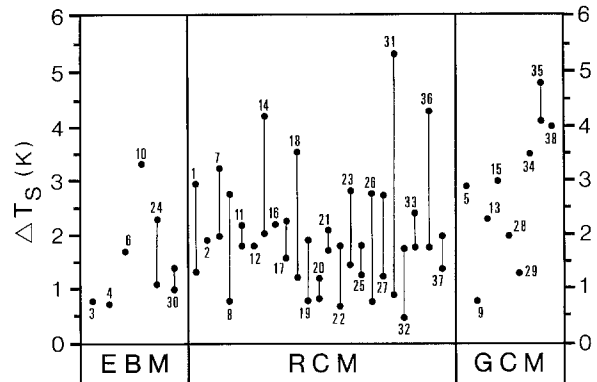


Fig. 1. The change of surface air temperature for doubling ($2 \times \text{CO}_2$) the CO₂ concentration as simulated by energy balance models (EBMs), radiative-convective models (RCMs) and general circulation models (GCMs). This figure is adapted and modified from Schlesinger (1984). References 9 and 13 are zonal mean dynamical models.

1 Manabe and Wetherald (1967); 2 Manabe (1971); 3 Rasool and Schneider (1971); 4 Weare and Snell (1974); 5 Manabe and Wetherald (1975); 6 Temkin and Snell (1976); 7 Augustsson and Ramanathan (1977); 8 Rowntree and Walker (1978); 9 Ohring and Adler (1978); 10 Ramanathan et al. (1979); 11 Hunt and Wells (1979); 12 Ackerman (1979); 13 Potter (1980); 14 Wang and Stone (1980); 15 Manabe and Wetherald (1980); 16 Ramanathan (1981); 17 Charlock (1981); 18 Hansen et al. (1981); 19 Hummel and Kuhn (1981a); 20 Hummel and Kuhn (1981b); 21 Hummel and Reck (1981); 22 Hunt (1981); 23 Wang et al. (1981); 24 Chou et al. (1982); 25 Hummel (1982a); 26 Hummel (1982b); 27 Lindzen et al. (1982); 28 Schlesinger (1983); 29 Washington and Meehl (1983); 30 Adem and Garduno (1984); 31 Wang et al. (1984); 32 Somerville and Remer (1984); 33 Lal and Ramanathan (1984); 34 Washington and Meehl (1984); 35 Hansen et al. (1984); 36 Ou and Liou (1985); 37 Gutowski et al. (1985); 38 Wetherald and Manabe (1986)

Gates et al. 1981) giving temperature changes considerably smaller than those of the GCMs computing the oceanic surface temperature explicitly. Also, we do not report the large (Moller 1963; Kandel 1981) and small sensitivities (Newell and Dopplick 1979; Idso 1980) obtained by EBMs using an energy balance for the Earth's surface rather than for the entire Earth-atmosphere climate system. This is justified on the basis of recent work by Schlesinger (1985) and Luther and Cess (1985) who have analysed the surface energy balance approach to estimate climate sensitivity. More particularly, Schlesinger (1985) has presented a generalized energetical formulation applying to surface and planetary EBMs. Within this framework, he has highlighted the inability of surface EBMs in general to determine simply the behaviour of the climate system away from the surface energy balance level.

From Fig. 1 we can conclude that the range of the warming obtained by GCM simulations (ex-

cluding zonally averaged dynamical models) for a doubling of CO₂, i.e. 1.3–4.8 K, is similar to that of RCMs (1-D and 2-D) and slightly greater than that of EBMs (1-D and 2-D). Indeed, the simulated warming by EBMs ranges from 0.7 to 3.3 K, while the range of the warming obtained by RCM simulations is 0.5–5.3 K.

Clearly, although a doubling in atmospheric carbon dioxide is expected to lead to a warming of the troposphere and of the Earth's surface, the estimates of this temperature increase are highly dependent on the physical assumptions made in the model. For example, using a RCM, Augustsson and Ramanathan (1977) have found an increase of 2 K with fixed cloud-top altitudes, but 3.2 K if cloud-top temperatures are held constant. With the same kind of model, Hansen et al. (1981) observed that, depending on the precise formulation and on the feedbacks included, the resultant change in surface temperature varies between 1.2 and 3.5 K.

As far as general circulation model (GCM) experiments are concerned, the series of Manabe and colleagues' (GFDL) experiments best illustrates the sensitivity of the predicted global warming, and particularly the warming at high latitudes, to variations in the assumed experimental conditions. As the assumptions were made more realistic in the GFDL GCMs (e.g., topography, land/ocean distribution, seasonal insolation), the sensitivity of the global surface temperature tended to decrease, reaching a value of about 2 K [inferred from the quadrupling experiment of Manabe and Stouffer (1980), noted GFDL1]. However, this is not confirmed by the last GFDL simulation (Wetherald and Manabe 1986, noted GFDL2), which includes an interactive cloudiness contrary to GFDL1, and by two other recent GCMs: the NCAR model (Washington and Meehl 1984) and the GISS model (Hansen et al. 1984). Like GFDL1 and GFDL2, these two models include a realistic geography, a global computational domain, nine layers along the vertical, sea-ice prediction, cloud prediction (except GFDL1), seasonal cycle of insolation and a mixed ocean layer without meridional oceanic heat transport (except GISS which uses prescribed heat transport). For a doubling of CO₂, GFDL1, GFDL2, NCAR and GISS give a global annual mean surface warming of 2 K, 4 K, 3.5 K and 4.2 K, respectively. All these models agree in simulating the largest warming in high-latitude regions over polar sea ice during winter.

However, these results are not conclusive because there are large sources of uncertainty in

modelling the feedback effects from clouds and sea-ice extent changes. As explained by Dickinson (1985), the GFDL1 response is probably underestimated because the sea-ice extent in the control run is too small. The NCAR2 response, on the contrary, is probably overestimated because the sea-ice extent in the control run is too large, and the largest GISS response is critically dependent on the cloudiness changes predicted by the model. Schlesinger and Mitchell (1985) emphasize also that the feedback of the predicted clouds in the GFDL2 experiment apparently almost doubles the global sensitivity of the surface temperature change (compare GFDL1 and GFDL2 sensitivities to a CO₂ doubling). Further, none of these GCMs used a fully coupled ocean – atmosphere system (including the vertical transport of heat associated with the large-scale upwelling and downwelling of water) and the parameterizations of many land or ocean surface processes are very crude. As an example, the need to include the dynamics of sea ice (ignored in all present GCM simulations), as well as its thermodynamics, has been discussed by Hibler (1984) who concluded that the poleward amplification of a CO₂-induced warming may not exist in a climate model simulation when sea-ice dynamics are included.

Besides GCMs and 1-D models, a few two-dimensional (2-D) dynamic or heat balance models have been designed in the recent past to study the role of particular feedback mechanisms in the CO₂ problem. Ohring and Adler (1978), Potter (1980), Chou et al. (1982), Ou and Liou (1984) and Wang et al. (1984) have presented results using latitude-altitude models, while Adem and Garduno (1984) and North et al. (1984) used latitude-longitude models. Their results are not contradictory to GCM simulations. Indeed, such intermediate climate models are thought to be complementary to GCM experiments by investigating in a simpler way the role of various feedbacks and by serving as guides for experimentation with the more comprehensive models. Moreover, climate simulation with GCMs requires exceedingly large amounts of computer time, which can seriously limit their use for climate dynamics studies. This is especially true for the investigation of long-term climatic changes because of the very different time scales of atmospheric, oceanic and cryospheric variations and of changes in the characteristics of the underlying land and sea surfaces.

Finally, the potential importance of other feedbacks, which are presently not included in usual climate models, has recently been further

assessed with simple climate models. Using 1-D RCMs, Charlock (1982) and Somerville and Remer (1984) have obtained a generally negative feedback (up to around 50% for the latter authors) by relating in simple fashions the cloud liquid-water-content change (which in these models give the cloud optical depth change) to the air temperature variation at the cloud level. The cloud optical properties are also related to the cloud droplet distributions and the cloud condensation nuclei concentrations. Twomey et al. (1984) have deduced, from measurements of particulate short-wave absorption and nucleus concentration, that observed increasing pollution levels over the North Atlantic give mainly optically thicker and more reflecting cloud layers, i. e., a cooling effect. They concluded that, in the next 50–100 years, the global climatic effect of (supposed) pollution increases could be quite comparable in absolute value to that of CO₂ increase but acting in the opposite direction. Even though preliminary [see comment papers by Heintzenberg and Ogren (1985) and by Bohren (1985)], these recent works provide further evidence that cloud-radiation interactions are fundamental in climate sensitivity modelling (and not only through cloud-extent changes). Clearly more studies and observational research are needed to confirm the negative feedbacks proposed in these studies.

In conclusion, two major problems still arise, at least in equilibrium climate research: namely,

the treatment of the ocean (including sea-ice) and of clouds. Fully coupled ocean-atmosphere general circulation models begin to exist but they are expensive to run to equilibrium due to the large thermal inertia of the deep ocean. On the other hand, whereas one can predict with reasonable confidence that the ocean temperatures will rise with increased CO₂, it is still difficult to predict the accompanying change in global cloudiness and in cloud optical properties. Nevertheless, GCM results, as shown in Fig. 1, turn out to converge on approximately the same conclusion: doubling the pre-industrial CO₂ concentration (up to about 550 ppmv), which could occur during the second half of the twenty-first century (UNEP-WMO-ICSU 1985), will correspond to a global equilibrium warming of 2–4 K.

As indicated in the Introduction, the change in concentration of other trace gases can reinforce the CO₂-induced climatic change in the near future. Today, published climate model calculations for various increases in trace gas concentration indicate a possible global mean surface warming comparable to that of CO₂ over the next 50–100 years (Volz 1983; Ramanathan et al. 1985; Wang and Molnar 1985; Lal et al. 1986; Wang et al. 1986). In fact, a simple way to estimate the climatic effect of trace gases (including CO₂) is to define, following the suggestion of Flohn (1978), an equivalent CO₂ concentration (because of similar greenhouse effect-climate interactions for

Table 1. Estimates of global surface air temperature changes resulting from variations in trace gas concentration. These results have been obtained using radiative-convective models with a fixed critical lapse rate of 6.5 K/km and fixed cloud-top altitude (from Wang et al. 1976; WMO 1983 a; and Ramanathan et al. 1985)

Constituent	Mixing ratio change (ppbv)		Surface temperature change (K)
	From	To	
CO ₂ (carbon dioxide)	3×10^5	6×10^5 (2 ×)	2.0
N ₂ O (nitrous oxide)	300	375 (1.25 ×)	0.12
CH ₄ (methane)	1650	2062 (1.25 ×)	0.09
CFCl ₃ (CFC-11)	0	1	0.14
CF ₂ Cl ₂ (CFC-12)	0	1	0.16
CF ₃ Cl (CFC-13)	0	1	0.22
CF ₂ HCl (CFC-22)	0	1	0.04
CHCl ₃ (Chloroform)	0	1	0.06
CH ₂ Cl ₂ (methylene chloride)	0	1	0.03
CH ₃ CCl ₃ (methyl chloroform)	0	1	0.02
CCl ₄ (carbon tetrachloride)	0	1	0.08
CF ₄ (carbon tetrafluoride)	0	1	0.06
NH ₃ (ammonia)	0	1	0.09
HNO ₃ (nitric acid)	present concentration	2 ×	0.06
Tropospheric O ₃	idem	1.5 ×	0.4
Total O ₃	idem	0.75 ×	-0.34
Stratospheric H ₂ O	3000	6000	0.6

each trace gas). The relative importance of all trace gases except CO₂ is highlighted by considering the time period from present to reach a doubled pre-industrial CO₂ concentration: UNEP-WMO-ICSU (1985) gives 100 years (around 2075) for CO₂ concentration alone and 50 years (around 2030) for equivalent CO₂ concentration, assuming particular scenarios for trace-gas concentration changes. We will introduce an equivalent CO₂ concentration in the next sections. To illustrate the relative importance of various trace gases, Table 1 gives an estimate of the change in equilibrium surface temperature for hypothetical concentration changes. These results have been obtained with RCMs assuming a fixed cloud-top height and a fixed critical lapse rate of 6.5 K/km.

In the next section, we introduce a simple formulation to estimate the effect on global equilibrium temperature of a specific radiative forcing. The results of such a simple formulation will be compared with the results discussed in this section.

Simple estimate of the global equilibrium temperature change for a radiative forcing

Let us consider the global-mean surface temperature as the climatic variable. As induced by an initial radiative perturbation ΔQ_T , the change of the surface temperature after a time period long compared to the thermal relaxation times within the climate system (i.e. at equilibrium) can be approximated by the following simple expression (e.g. Lal and Ramanathan 1984; Cess 1985):

$$\Delta T_e = \frac{\Delta Q_T}{\lambda}. \quad (1)$$

In Eq. (1), ΔQ_T is the initial radiative heating perturbation of the surface-troposphere system, i.e., the radiative perturbation at the tropopause before any response of the climatic system. λ is the climate feedback parameter (Dickinson 1982) defined as

$$\lambda = \frac{d(IR)^N}{dT_e} + \frac{dS^N}{dT_e}$$

where $(IR)^N$ and S^N are the net infrared and solar fluxes, respectively, at the top of the atmosphere, with $X^N = \text{upward } X - \text{downward } X$. This parameter quantifies the atmospheric radiative damping

due to the feedback processes in the climate system and determines its global response to a given external radiative perturbation ΔQ_T .

The assumption behind Eq. (1) is that the surface-troposphere system responds as a single coupled thermodynamic system if λ is independent of the type and magnitude of the forcing. Therefore, the λ value would depend only on the climate model. Cess et al. (1985) analysed this assumption with a global RCM and concluded that Eq. (1) gives a correct estimate of the global surface temperature response to a doubled CO₂ concentration and to small solar constant changes for which initial warmings occur both in the troposphere and at the surface, but is not adapted to radiative perturbations such as that involved in nuclear war scenarios where absorbing smoke ejected by large-scale fires implies an initial warming of the troposphere but a cooling of the surface.

For trace-gas-induced climatic change in the near past and future, Eq. (1) is thought to be valid to give a first-order estimate of the equilibrium surface temperature response because, for such climatic perturbations, the surface and the troposphere will most probably remain strongly coupled by radiative and non-radiative processes including transfer of latent and sensible heat by convective and advective heat transports. Therefore, here we will assume the surface warming to be linked to the trace-gas-induced radiative perturbation at the tropopause ΔQ_T . We now have to specify the change in the heat balance (ΔQ_T) due to change in the considered external parameter (e.g., CO₂ concentration) and the climate system change in response to a given ΔQ_T (λ value).

From semi-empirical and various model studies discussed in Dickinson (1982, 1985), we concluded that the most reasonable range of values for λ would be:

$$\lambda = 1.8 \pm 1.0 \text{ Wm}^{-2} \text{ K}^{-1}. \quad (2)$$

On the other hand, for a CO₂ doubling, radiative calculations (Kiehl and Ramanathan 1982; Wang and Ryan 1983; Lal and Ramanathan 1984) give:

$$\Delta Q_T(2 \times \text{CO}_2) = 4.2 \pm 0.3 \text{ Wm}^{-2}. \quad (3)$$

Using this range of radiative perturbations and the λ values given by relation (2), the following range of estimates is obtained through Eq. (1) for the equilibrium surface temperature response to a CO₂ doubling:

$$\Delta T_e(2 \times \text{CO}_2) = 3.5 \pm 2.1 \text{ K}, \quad (4)$$

i.e., a temperature increase ranging from 1.4 to 5.6 K. This range is similar to the range of most expected warming as given by the Villach UNEP-WMO-ICSU (1985) report and near the range of 0.5–5.3 K given in Fig. 1 by making a selection among the published model results for a CO₂ doubling. Moreover, differences between these ranges can be explained by values of λ and/or ΔQ_T , used in some selected models, being outside the values defined by Eqs. (2) and (3), respectively.

Scenarios for trace-gas concentration changes and equilibrium response

The actual potential trace-gas-induced climatic change involves continuously varying trace gas concentrations. Even so, Eq. (1) can be used to estimate in a simple way the instantaneous associated equilibrium surface temperature response if the time-dependent forcing $\Delta Q_T(t)$ is further specified. Usually rather arbitrary scenarios regarding the past and future variations in trace gas concentrations were chosen solely for the purpose of illustrating how the climate could respond to a change in such concentrations. The use of different scenarios in different models leads to differences in results that are not always easily understood or explained. Recently, Wuebbles et al. (1984) have analysed in detail the problem of the choice of past and future scenarios for trace gas concentrations. For a few radiatively active atmospheric constituents, they have proposed a reference set of such past and future scenarios which could be homogeneously adopted for transient studies in the future, allowing better intercomparisons between models.

Therefore, in this paper, the past and future scenarios of trace gas concentrations have been taken from the various sets of scenarios proposed by Wuebbles et al. (1984). For CO₂, CH₄ and N₂O, our scenarios correspond to those recommended as standard for most model calculations by these authors (see Table 2 and Fig. 2a–c). In Fig. 2a the high and low post-1983 emission scenarios for CO₂ are also given as proposed by Wuebbles et al. as extreme growth scenarios for use in modelling studies. In all CO₂ scenarios given in Fig. 2a, a pre-industrial concentration of 270 ppmv has been assumed (WMO, 1983b; Raynaud and Barnola, 1985) although the value given by Neftel et al. (1985) is near 290 ppmv and the range given by UNEP-WMO-ICSU (1985) is 275 ± 10 ppmv. For the chlorocarbons CFC₁₃,

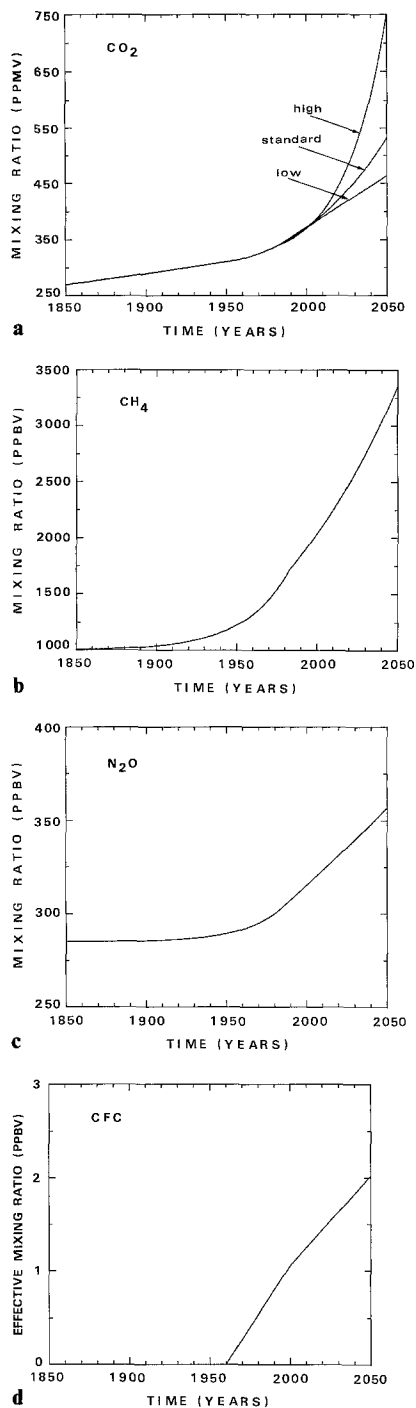


Fig. 2a–d. a CO₂ volume mixing ratio (in ppmv) as a function of time for standard, high and low scenarios (see also Table 2). b CH₄ volume mixing ratio (in ppbv) as a function of time for the scenario given in Table 2. c as in b but for N₂O. d as in b but for equivalent chlorocarbon

CF₂Cl₂, CF₂HCl, CH₃CCl₃ and CCl₄, the results of the Lawrence Livermore National Laboratory 1-D photochemical model, given by Wuebbles et al. and computed from historical CFC emissions,

are used and future scenarios assume constant surface emission at the 1983 rates. In our computation, only a global radiatively weighted mean chlorocarbon concentration variation $\Delta C[\text{CFC}]$ is used and defined by (see Appendix):

$$\begin{aligned} \Delta C[\text{CFC}]_t = & (\Delta C[\text{CF}_2\text{Cl}_2] \\ & + 0.873 \Delta C[\text{CFCl}_3] \\ & + 0.5 \Delta C[\text{CCl}_4] \\ & + 0.114 \Delta C[\text{CH}_3\text{CCl}_3] \\ & + 0.283 \Delta C[\text{CF}_2\text{HCl}]), \end{aligned} \quad (5)$$

where $C[X]$ is the concentration of the component X at time t , in ppbv, and $\Delta C[X] = (C[X] \text{ at time } t) - (C[X] \text{ at the initial time } t_0)$.

Table 2 gives the time-dependent scenario of this equivalent CFC concentration (assuming $C[\text{CFC}]_{1850} = 0$) and Fig. 2d illustrates this scenario.

The report of Wuebbles et al. (1984) is recommended for an extensive discussion of these scenarios and their uncertainties. Clearly, updated scenarios could be used in the future, but at the present time this set of scenarios is probably the most convenient for time-dependent computations. Knowing the time-dependent trace-gas concentration variations, the time-dependent forcing $\Delta Q_T(t)$ must now be determined.

The following approximate relation for CO_2 concentration change can be derived from Ramanathan et al. (1979):

$$\begin{aligned} \Delta Q_{\text{CO}_2}(t) = & \Delta Q_{\text{CO}_2}(2 \times) \\ & \times \ln(C[\text{CO}_2]_t / C[\text{CO}_2]_{t_0}) / \ln 2 \end{aligned} \quad (6)$$

where $C[\text{CO}_2]_t$ is the CO_2 concentration at time t ; $C[\text{CO}_2]_{t_0}$ is the initial CO_2 concentration at time t_0 ; $\Delta Q_{\text{CO}_2}(2 \times)$ is the radiative perturbation for a doubled CO_2 concentration.

This formulation is valid for concentration changes up to about four times the present CO_2 concentration; it is no longer realistic for larger concentrations (Augustsson and Ramanathan 1977).

Following the procedure of Wigley (1985), Eq. (6) can be modified to include approximately the effect of concentration changes of a set of other important trace gases, i.e. CH_4 , N_2O and chlorocarbons. An equivalent CO_2 concentration is thus introduced in order to include the time-dependent variation of all the trace gases by defining (see Appendix):

$$\begin{aligned} \tilde{C}[\text{CO}_2]_t = & C[\text{CO}_2]_t \exp \{0.00599 \\ & (\sqrt{C[\text{CH}_4]_t} - \sqrt{C[\text{CH}_4]_{t_0}}) \\ & + 0.01812 (\sqrt{C[\text{N}_2\text{O}]_t} - \sqrt{C[\text{N}_2\text{O}]_{t_0}}) \\ & + 0.05139 (C[\text{CFC}]_t)\}. \end{aligned} \quad (7)$$

Table 2. Time-dependent past and future scenarios for the trace gas concentrations taken from Wuebbles et al. (1984). The radiatively averaged concentration of chlorocarbons, CFC, is defined in the text; t is time in years and C is concentration in ppmv for CO_2 and in ppbv for other gases

Concentration		Trace gaz
From	To	Time-dependent
		CO_2
$t_0 = 1850$	1958	$C = 270 \exp[1.41 \times 10^{-3}(t - t_0)]$
$t_0 = 1958$	1983	$C = 270 + 44.4 \exp[1.9 \times 10^{-2}(t - t_0)]$
$t_0 = 1983$	2050	$C = 341.4 + 1.539(t - t_0) \exp[9.173 \times 10^{-3}(t - t_0)]$
		CH_4
1850	1983	$C = 1000 + 650 \exp[3.5 \times 10^{-2}(t - 1980)]$
$t_0 = 1983$	2050	$C = 1.720(1.01)^{(t - t_0)}$
		N_2O
1850	1983	$C = 285 + 14.0 \exp[4 \times 10^{-2}(t - 1978)]$
$t_0 = 1983$	2050	$C = 302.1(1.0025)^{(t - t_0)}$
		Radiatively averaged CFC
1850	1960	$C = 0$
$t_0 = 1960$	1983	$C = 0.0268(t - t_0)$
$t_0 = 1983$	2000	$C = 0.615 + 0.026(t - t_0)$
$t_0 = 2000$	2050	$C = 1.057 + 0.019(t - t_0)$

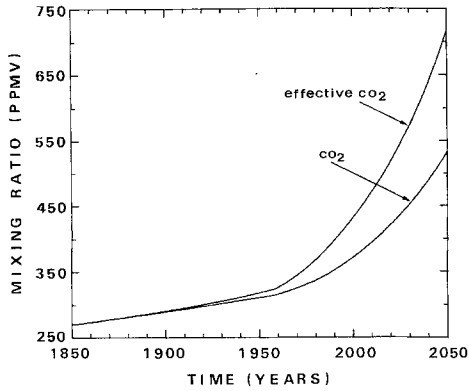


Fig. 3. Volume mixing ratio (in ppmv) as a function of time. The *upper curve* represents the evolution of the effective (also called virtual by Flohn 1978, and equivalent in the text) CO₂ concentration, $\bar{C}[\text{CO}_2]$, and the *lower curve* represents the evolution of the CO₂ concentration alone, $C[\text{CO}_2]$. These curves are for the standard CO₂ scenario given in Fig. 2 a

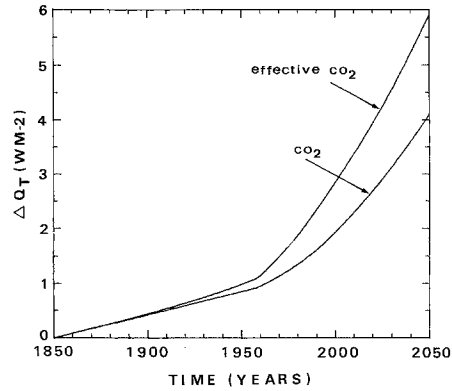


Fig. 4. Radiative flux perturbation at the tropopause (ΔQ_T) as a function of time. The *upper curve* represents the perturbation induced by the variation of the effective CO₂ concentration and the *lower curve* represents the perturbation induced by the variation of the CO₂ concentration alone. These curves are for the standard CO₂ scenario given in Fig. 3

For our standard scenarios, Fig. 3 gives the time-dependent CO₂ and equivalent CO₂ concentrations (CO₂ + other trace gases) from 1850 to 2050. An interesting feature of Fig. 3 is the rapid equivalent CO₂ concentration increase after 1960 due to the important release of trace gases in the atmosphere. A similar behaviour was obtained by Wigley (1985) with slightly different past and future scenarios. It is worth noting that our standard scenarios give a doubled CO₂ concentration in 2052 and a doubled equivalent CO₂ concentration in 2025 [2052 is also given by the upper-bound CO₂ scenario selected in the UNEP-WMO-ICSU report (1985); for the equivalent CO₂ concentration, 2025 is very close to the standard date given in the same report].

Using Eq. (7) with the scenarios we have selected, the equivalent radiative perturbation ΔQ_T (see Fig. 4) is obtained, allowing an estimate with Eq. (1) of the instantaneous equilibrium surface temperature response if the value of the feedback climate parameter λ is specified.

To test the accuracy of our approximate radiative treatment, our results were compared to those of Ramanathan et al. (1985) by using their model response to a doubling of CO₂ (~1.9 K) and their trace gas concentrations for the time periods 1880–1980 and 1980–2030. For the year 2030, these authors proposed a standard concentration similar to ours for CO₂ (450 ppmv), a smaller value for CH₄ (2340 ppbv instead of 2750 ppbv), larger values for N₂O (375 ppbv instead of 340

Table 3. Contributions of the various trace gases to the equilibrium surface warming for the 1880–1980 and 1980–2030 periods. *Row A* gives the results of Ramanathan et al. (1985) obtained with sophisticated radiative calculations. *Row B* gives the results obtained from our radiative computations, using the same scenarios as Ramanathan et al.. *Row C* gives the results of our radiative computations using the standard scenarios proposed by Wuebbles et al. (1984). The results given in rows B and C have been obtained using a model sensitivity to a CO₂ doubling similar to that of Ramanathan et al. (~1.9 K) for the purpose of the present comparison

	ΔT_e (1880–1980)					ΔT_e (1980–2030)				
	CO ₂	CH ₄	N ₂ O	CFC	Total	CO ₂	CH ₄	N ₂ O	CFC	Total
A. Ramanathan et al. (1985)	0.52	0.12	0.02	0.09	0.75	0.71	0.14	0.10	0.43	1.37
B. This study (Ramanathan et al. scenarios)	0.61	0.11	0.02	0.07	0.82	0.77	0.13	0.10	0.40	1.39
C. This study (standard scenarios)	Same as in B because trace gas concentrations in Ramanathan et al. (1985) and in this study are the same					0.80	0.19	0.06	0.16	1.21

ppbv) and larger effective chlorocarbon CFC (3.3 ppbv instead of 1.6 ppbv). The comparison of the first and second rows of Table 3 indicates that the present radiative formulation overestimates the CO₂-induced warming by 17% and 8% (for the first and second periods, respectively), underestimates the CH₄-induced warming by ~10%, gives similar results for N₂O and underestimates the CFC-induced warming by 7% and 22%. Globally, our radiative treatment overestimates the warming by 10% for the 1880–1980 period and gives a similar result for the 1980–2030 period. For the latter period, the third row of Table 3 gives results using our radiative formula and the standard scenarios selected for this study instead of those of Ramanathan et al. Comparing rows 2 and 3, the differences in trace gas scenarios lead to a difference between the temperature responses which amounts to 0.2 K in 2030, the largest temperature response being obtained with the scenarios of Ramanathan et al. This means that the impact of their larger future equivalent CFC concentration prevails over their smaller future CH₄ concentration. Let us also remark that CH₄ and chlorocarbons have a rather similar climatic impact in the future if the scenarios of Wuebbles et al. are adopted, whereas the scenarios proposed by Ramanathan et al. give a larger climatic importance to the chlorocarbons (actually the largest after CO₂).

Furthermore, within the simple framework defined here, we can readily estimate the historical relative importance of CO₂ and all other trace gases. Using the ranges given by Eqs. (2) and (3), Table 4 gives the ranges for the radiative perturbation and the equilibrium temperature increase between the pre-industrial time and the present. The results are shown for CO₂ alone and for equivalent CO₂, and for two pre-industrial CO₂ concentrations. For the standard pre-industrial CO₂

Table 4. Radiative perturbations at the top of the atmosphere (ΔQ_T) and equilibrium surface warming (ΔT_e) between the pre-industrial time (1850) and the present (1980). Estimates are given for two pre-industrial CO₂ concentrations (270 and 290 ppmv), and for CO₂ alone and CO₂ + other trace gases included in the present study (equivalent CO₂)

	Pre-industrial CO ₂	
	270 ppmv	290 ppmv
$\Delta Q_T(\text{CO}_2)$ (Wm^{-2})	1.4 ± 0.1	1.0 ± 0.1
$\Delta Q_T(\text{equivalent CO}_2)$ (Wm^{-2})	2.0 ± 0.1	1.5 ± 0.1
$\Delta T_e(\text{CO}_2)$ (K)	1.2 ± 0.7	0.8 ± 0.5
$\Delta T_e(\text{equivalent CO}_2)$ (K)	1.7 ± 1.0	1.3 ± 0.8

concentration of 270 ppmv, Table 4 shows a mean equilibrium temperature increase of 1.7 K for the equivalent CO₂, with a relative contribution from all trace gases except CO₂ of 40% (0.5 K) by comparison to the contribution from CO₂ alone (1.2 K). For a pre-industrial CO₂ concentration of 290 ppmv, Table 4 now shows a mean equilibrium temperature increase of 1.3 K for the equivalent CO₂, with a relative contribution from all trace gases except CO₂ of 60% by comparison with the new contribution from CO₂ alone (0.8 K). But, as shown above, our approximate radiative treatment overestimates the CO₂-induced radiative perturbation by ~15% and similarly underestimates the role of the other trace gases. The relative contributions of different trace gases are therefore only approximate and are given here just as illustrations.

To complete these equilibrium computations, Fig. 5 gives the global equilibrium temperature changes from 1850 to 2050, using our standard scenarios and three model responses of 1 K, 3 K and 5 K, respectively, for a CO₂ doubling (ΔQ_T is fixed at 4.2 Wm^{-2}). Since the pre-industrial time, the expected temperature increase ranges between 0.5 and 2.2 K in 1980, between 0.8 and 4.0 K in 2010, and between 1.4 and 7.0 K in 2050.

Figure 5 has been obtained for the standard future CO₂ scenario. Combining the three model responses for a CO₂ doubling and the three future CO₂ scenarios given in Fig. 2a would give temperature increases between 0.8 and 4.1 K in 2010 and between 1.2 and 9.5 K in 2050. The difference between the future CO₂ concentrations given by Wuebbles et al. (1984) leads to significant differences between the equilibrium temperature responses only after 2010.

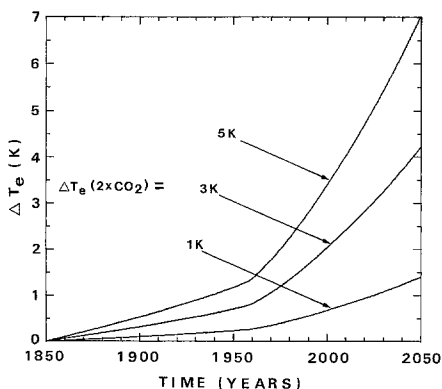


Fig. 5. Time-dependent response of the equilibrium surface temperature (ΔT_e) for the time-dependent radiative perturbation (ΔQ_T , for equivalent CO₂) shown in Fig. 4. The three curves are given for $\Delta T_{ac}(2 \times \text{CO}_2) = 1 \text{ K}, 3 \text{ K}$ and 5 K

The equilibrium computations presented here are not thought, even in a simple way, to give the actual time-dependent response of the global climate system to CO₂ and other trace-gas-induced radiative perturbations. Their principal interest was only to clarify the notion of the radiative perturbation and of the climate feedback parameter. Indeed, because of the heat capacity of the oceans, the climate system cannot be in equilibrium with the current trace gas concentrations. As a consequence, neglecting the oceanic thermal inertia does not allow models to reproduce the time delay which can be anticipated for the trace-gas-induced global warming. In the next section, the role of the ocean's buffering will be discussed in relation to the transient response of the climate system to radiative forcing.

Modelling the transient response

Description of the global model

To estimate the time-dependent response of the climate system to time-dependent trace-gas concentration changes, various simplified sets of global time-dependent energy budget equations can be used (e.g., Hoffert et al. 1980; Wigley and Schlesinger 1985; Harvey and Schneider 1985a, 1985b).

One particularly simple set of such equations can be obtained by considering only two globally and annually averaged coupled atmosphere and ocean boxes. The following equations can be written for the atmosphere (*a*) and the surface (*s*), respectively (Harvey and Schneider 1985a):

$$\rho_a c_{pa} \Delta Z_a \frac{\partial \Delta T_a}{\partial t} = \Delta LE + \Delta H + \Delta F_n - \Delta F_a \uparrow \quad (8)$$

$$\rho_s c_{ps} \Delta Z_s \frac{\partial \Delta T_s}{\partial t} = -\Delta LE - \Delta H - \Delta F_n - r \Delta F_{sd} \quad (9)$$

where ΔX means the departure of *X* from its fixed equilibrium value; ρ_i , c_{pi} , ΔZ_i , T_i are the density, heat capacity, depth and temperature of the reservoir *i* (*i* = *a* or *s*), respectively; LE , H and F_n are the heat transfers from the surface to the atmosphere due to latent heat, sensible heat and net long-wave radiation at the surface, respectively; $F_n = F_s^\uparrow - F_s^\downarrow$ with F_s^\uparrow and F_s^\downarrow the upward long-wave radiation emitted by the surface and the downward long-wave radiation, respectively; F_a^\uparrow is the upward long-wave radiation at the top of the atmosphere; F_{sd} is the heat transfer between

the mixed layer and the deeper ocean [the parameterization of this term will be discussed later, to close the system given by Eqs. (8) and (9)]; r is the fraction of the Earth's surface covered by oceans (0.71).

In Eq. (9), ΔZ_s is an equivalent layer depth, obtained by taking a particular weighting of the actual mixed layer and land inertia. This equivalent mixed-layer depth allows the effect of the smaller land heat capacity to be included, assuming a finite wind mixing between the oceanic and continental atmospheres (Harvey and Schneider 1985a).

In the next sections, time-dependent results will be presented using Eqs. (8) and (9) with the following heat flux parameterizations:

$$F_s^\uparrow = \sigma T_s^4 \quad (10)$$

$$F_s = \varepsilon \sigma T_a^4 \quad (11)$$

$$H = C_H (T_s - T_a) \quad (12)$$

$$LE = C_{LE} (e_s - e_a) \quad (13)$$

$$F_a^\uparrow = A + B T_a \quad (14)$$

where σ is the Stefan-Boltzmann constant; ε is the equivalent emissivity of the sky given by Centuno (1982) as a function of cloudiness n , T_a and relative humidity RH of the surface air; C_H and C_{LE} are the drag coefficients for the sensible and latent heat fluxes, respectively; e_s is the saturation water vapour pressure at surface temperature T_s ; e_a is the atmospheric water vapour pressure using a fixed relative humidity RH .

In all our simulations, the surface and atmospheric solar absorptions have been assumed fixed, giving a constant planetary albedo equal to 0.31 for a solar constant of 1368 Wm⁻². On the other hand, in the parameterization of F_a^\uparrow we can simulate the radiative effect of trace gas changes (i.e. a change of atmospheric opacity) by modifying the value of the constant A in Eq. (14) (Harvey and Schneider 1985a). With these assumptions and reintroducing the simple equilibrium formulation given earlier, it can be shown that we have

$$-\Delta A = \Delta Q_T \text{ and } \lambda = B. \quad (15)$$

Therefore, in the global model given by Eqs. (8) and (9), the climatic feedback parameter λ is an

adjustable parameter given by the chosen value of B in the parameterization of the upward infrared flux at the top of the atmosphere. For a particular choice of B , an equation similar to Eq. (1) gives directly the equilibrium surface air (not surface) temperature response of the model, ΔT_{ae} , for a given radiative perturbation ΔQ_T . ΔQ_T is assumed to be totally included in the atmosphere, neglecting the accompanying variation of F_s^l . Harvey and Schneider (1985b) have shown the validity of such an approximation in their model.

To solve Eqs. (8) and (9), the formulation of the heat exchange between the mixed layer and the deeper ocean must be explicitly formulated. Such heat transport results mainly from motion along constant-density (isopycnal) surfaces at low latitudes and convective overturning in the North Atlantic and Antarctic basins (e.g., Garrett 1979). Two simplified formulations have generally been proposed which hopefully incorporate the global effect of numerous heterogeneous regional mixing processes. The first usual formulation is obtained by using an advection-diffusion equation for the heat penetration in the deeper ocean. It is assumed that, on a global scale, the vertical mixing in the ocean interior can be parameterized as

$$F_{sd} = \rho_s c_{ps} \left[K \frac{\partial T_d}{\partial Z} + W (T_d - T_B) \right]_{Z=0} \quad (16)$$

where T_d is the horizontally averaged deep ocean temperature below the mixed layer, T_B is the bottom water temperature (~ 1.2 K), $Z=0$ is the level of the bottom of the mixed layer ($Z>0$ in the deeper ocean), K is a constant vertical eddy diffusion coefficient, W is a constant averaged upwelling velocity for the world ocean.

Equation (16) is obtained by assuming that the polar water sinks with a constant temperature T_B and spreads instantaneously throughout the ocean bottom. Subsequently, this cold flow is brought to the surface by upwelling over the world ocean.

Equation (16) defines the so-called box advection-diffusion ocean model or BADOM (Hoffert et al. 1980; Harvey and Schneider 1985a; Watts 1985). To obtain the evolution of the deep ocean temperature, the following relation is used:

$$\frac{\partial T_d}{\partial t} = K \frac{\partial^2 T_d}{\partial Z^2} + W \frac{\partial T_d}{\partial Z} \quad (17)$$

with the boundary conditions

$$T_d = T_s \quad \text{at } Z=0$$

$$T_d = T_B \text{ or } K \frac{\partial T_d}{\partial Z} + W T_d = W T_B \quad \text{at } Z=D,$$

where D is the depth of the ocean bottom.

The steady-state solution of Eq. (17) is

$$T_d(Z) = T_B + (T_s - T_B) \exp\left(-\frac{K}{W} Z\right). \quad (18)$$

In equilibrium, the temperature profile of $T_d(Z)$ is adjusted such that the divergence of the upward advective heat flux balances the convergence of the downward diffusive heat flux at each point. Values of $W=4$ m year⁻¹ and $K=0.6$ cm²s⁻¹ have been proposed by Hoffert et al. (1980) to reproduce a vertical global temperature profile close to the GEOSECS (Geochemical Ocean Sections) world data.

In some other studies (e.g., Hansen et al. 1981; Siegenthaler and Oeschger 1984; Schlesinger et al. 1985), a purely diffusive [i.e., $W=0$ in Eqs. (16) and (17)] ocean model (BDOM) has been used for transient climate studies. In BDOM, the value of the eddy diffusion coefficient is usually calibrated against ocean geochemical data. For global modelling, only natural radiocarbon, bomb-produced radiocarbon and tritium distributions are available from GEOSECS data. Currently, the global tritium distribution is thought to provide the most valuable information. Li et al. (1984) have recently given a new estimate of the effective average vertical mixing coefficient for the oceanic thermocline equal to 1.7 cm²s⁻¹, based on all GEOSECS tritium data. Usually, the K values used in BDOM range between 1 and 3 cm²s⁻¹.

In the next section, the transient response obtained with the BADOM and BDOM formulations will be discussed and the questionable points in both formulations for modelling oceanic heat transfer will be mentioned briefly. A few particular results of some GCM experiments which have addressed the climate transient response to an instantaneous CO₂ increase will end our discussion.

Discussion of BADOM and BDOM formulations

Using the EBM formulation given by Eqs. (8) and (9), Harvey (1986) undertook numerical comparisons between BADOM and BDOM parameterizations for a fixed instantaneous CO₂ doubling. Comparing the model e -folding time τ_e (defined

as the necessary time period to reach 63% of the equilibrium response), he concluded that BADOM and BDOM have very different transient response characteristics. For diffusivity values K ranging between 1 and $10 \text{ cm}^2\text{s}^{-1}$, he showed that BADOM has a faster transient response than BDOM; such a difference had already been found and explained physically in Harvey and Schneider (1985a). He showed also that the transient response of BADOM cannot be reproduced with BDOM using the same effective K as BADOM, except during the first few decades of the transient response (here, for a fixed instantaneous CO_2 doubling). From his experiments, he concluded furthermore that the e -folding time cannot by itself meaningfully summarize the qualitative dependence of the transient response to ocean mixing parameters for the whole range of time scales between 1 and 1000 years. As a simple illustration of the qualitative and quantitative differences in time lag between BADOM and BDOM formulations, the transient response of both models will be presented in the next section for the time period 1850–2050 by using the time-dependent trace gas scenarios defined earlier. But before proceeding to such an experiment, the reliability of BADOM and BDOM for estimating the transient response in the real world must be addressed.

Hoffert and Flannery (1985) discussed the uncertainties of BADOM and BDOM formulations in detail. Clearly, BDOM does not describe the steady-state deep ocean, giving a constant vertical temperature profile equal to the steady-state oceanic mixed-layer temperature. Even if BDOM seems inadequate for looking at the transitions from one equilibrium state to another, such a model has been thought adequate for studying the response of the mixed layer to CO_2 forcing on a relatively short (≤ 100 years) time scale (Cess and Goldenberg 1981). Using an effective vertical diffusion coefficient derived from tracer data, BDOM assumes implicitly that the oceanic heat mixing can be parameterized as the effective oceanic isotopic tracer mixing. But, as explained by Hoffert and Flannery (1985) and by Harvey (1986), the effective vertical diffusivity derived from passive tracer data probably overestimates the vertical heat diffusion in the ocean. Indeed, tracer penetration into the upper ocean seems to occur mainly along isopycnals; whereas isopycnal mixing is less important in thermal diffusion because, on a global scale, isotherms are nearly isopycnals. Moreover, the effective diffusivity deduced from isotopic data is dependent on the ana-

lysed isotopic distribution. For example, Siegenthaler (1983) deduced a globally averaged K using the natural radiocarbon distribution which was about half that deduced using the bomb-produced radiocarbon distribution. The estimated value of K therefore depends strongly on the time scale involved (10 years for bomb-produced radiocarbon and more than 100 years for natural radiocarbon).

On the other hand, the K value in the BADOM formulation is based on the observed global temperature profile and the estimate of polar sinking flow. The effective diffusivity in BADOM therefore includes implicitly the effects of convection in the simulated equilibrium conditions. It is questionable that the convective activity will work at a rate similar to the present one if a heat perturbation occurs in the upper ocean.

Such questions could be addressed by some judicious oceanic GCM experiments. Current oceanic GCMs, however, do not resolve eddies at the scale at which much of the oceanic heat transport and mixing occurs, so that the results obtained with these models must still be considered as preliminary. We mention here briefly three examples of such oceanic GCM experiments. Bryan et al. (1984) assessed the use of the transient tracers in the ocean to deal with the downward penetration of a heat perturbation associated with a climatic change. They used an uncoupled oceanic GCM, in which a small positive surface temperature anomaly of 0.5 K was imposed, and made a numerical integration over a 50-year period to study the oceanic response. They found that the globally averaged vertical penetration of the heat perturbation could be reproduced rather satisfactorily with a box-diffusion ocean model. The efficiency of BDOM was explained by considering that small initial heat perturbations induced small buoyancy effects, which allowed the heat perturbations to behave as passive tracers.

Similarly, Schlesinger et al. (1985) used a box-diffusion ocean model with $K \sim 2.3 \text{ cm}^2\text{s}^{-1}$ to reproduce the globally averaged time evolution of the $(2 \times \text{CO}_2) - (1 \times \text{CO}_2)$ differences in the surface air and oceanic upper-layer temperatures computed with their coupled ocean-atmosphere GCM over a 16-year period. Incidentally, their globally averaged time-dependent vertical distribution of the oceanic temperatures up to 1550 m was also reproduced with a depth-variable eddy diffusion coefficient. The mass-weighted average of this eddy diffusion coefficient was $2.25 \text{ cm}^2\text{s}^{-1}$, in agreement with the values deduced from bomb-produced isotopic distributions. Ex-

trapolating the GCM results with the equivalent BDOM, the authors found that the e -folding time for the upper ocean was large (75 years). Based on his experiments comparing BADOM and BDOM time-dependent behaviour, Harvey (1986) questioned the extrapolation of BDOM results to time periods longer than a few decades. However, this remark is valid only if the vertical advection behaves as in BADOM for a heat perturbation, which is yet to be demonstrated.

In a third recent coupled ocean/atmosphere GCM experiment, Bryan and Spelman (1985) analysed the predicted response of the ocean over a 50-year period to a greater heat perturbation induced by a four-fold increase in atmospheric CO_2 . The effects of buoyancy become important in this study and a partial collapse of the thermohaline circulation of the ocean increases the heat storage of the deep ocean, producing a potential negative feedback for greenhouse warming. Harvey and Schneider (1985 a) have proposed another feedback, suggesting that the mixed-layer warming would increase the stability of the upper oceanic layers and could therefore diminish the diffusive penetration of heat. Unfortunately, the ocean model used by Bryan and Spelman (1985) does not allow a test of this potential positive feedback because the vertical diffusivity in the model is independent of the stability.

Progress in global eddy-resolving oceanic GCMs and time-dependent heat budget analysis of current oceanic GCMs (in particular, for determining the role of convection in transporting heat) could give a better assessment of the reliability of simple BDOM and BADOM to the study of the global transient response of the climatic system.

Transient climatic simulations of the past and future trace gas changes

In this section, our results of a few transient simulations are presented for a period extending from the pre-industrial time (defined as the year 1850) up to the middle of the next century (the year 2050). Our main goal is to illustrate the potential relative importance of some model uncertainties for the global climatic response. Unless mentioned, all simulations have been obtained using the global climate model described earlier coupled with an advective-diffusive deep ocean model (BADOM). Also, the time-dependent radiative forcing is normally estimated from the standard concentration scenarios given by Wue-

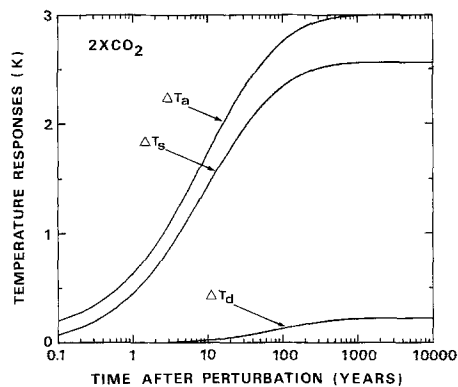


Fig. 6. Transient response of the EBM-BADOM model for an instantaneous CO_2 doubling. $\Delta T_{ae}(2 \times \text{CO}_2)$ is fixed at 3 K. ΔT_a , ΔT_s and ΔT_d are the surface air, the surface, and the vertically averaged deep ocean temperature responses, respectively

bles et al. (1984), following the procedure presented in an earlier section.

First of all, the e -folding time of the model has been given by the model transient response to the step-function forcing for an instantaneous CO_2 doubling (Fig. 6). Assuming an equilibrium increase of the surface air temperature [$\Delta T_{ae}(2 \times \text{CO}_2)$] equal to 3 K, we obtained e -folding times equal to 13 years and 14 years for the atmosphere and the equivalent mixed layer, respectively. Table 5 gives the value of the main parameters used in the model and Table 6 gives air and surface temperatures and some heat fluxes computed by the model for the present climate and for a CO_2 concentration doubling. From a set of simulations for a range of $\Delta T_{ae}(2 \times \text{CO}_2)$ between 1 K and 5 K, we found $\tau_e \propto \Delta T_{ae}^n(2 \times \text{CO}_2)$ with $n \sim 1.5$ for our present BADOM. From an analytical solution for an energy balance/box diffusion ocean model (BDOM), Wigley and Schle-

Table 5. Values of some parameters in the EBM-BADOM used in this study. A is given for the present climate (surface air temperature equal to 288 K) and assuming a surface air temperature increase of 3 K for a CO_2 doubling (also assumed for B)

Parameters	Values	In
K	$0.6 \text{ cm}^2 \text{ s}^{-1}$	Eqs. (16)–(17)
W	4 myr^{-1}	Eqs. (16)–(17)
C_H	$13.0 \text{ Wm}^{-2} \text{ K}^{-1}$	Eq. (12)
C_{LE}	$15.6 \text{ Wm}^{-2} \text{ K}^{-1}$	Eq. (13)
A	-168 Wm^{-2}	Eq. (14)
B	$1.4 \text{ Wm}^{-2} \text{ K}^{-1}$	Eq. (14)
RH	0.77	Eqs. (11)–(13)
n	0.55	Eq. (11)

Table 6. Steady-state global mean temperatures (in K) and heat fluxes (in Wm^{-2}) for the present climate and for a doubled CO_2 concentration. $2 \times \text{CO}_2$ values are given for a surface air temperature response equal to 3 K

	Present	$2 \times \text{CO}_2$
Temperature (K)		
air	288.0	291.0
surface	289.3	291.8
Sensible flux (Wm^{-2})	16.7	11.0
Latent flux (Wm^{-2})	83.1	90.5
Long-wave flux (Wm^{-2})		
downward at the surface	335.9	352.0
upward at the top	236.0	236.0
ΔQ_T (Wm^{-2})	—	4.2

singer (1985) obtained a τ_e depending quadratically on $\Delta T_{ae}(2 \times \text{CO}_2)$. Suppressing the upwelling flow in our BADOM formulation, we found $\tau_e = 17$ years for the atmosphere when $\Delta T_{ae}(2 \times \text{CO}_2) = 3$ K and $\tau_e \propto \Delta T_{ae}^n(2 \times \text{CO}_2)$ with $n \sim 1.7$ for model sensitivities ranging between 1 K and 5 K. These results are thus consistent with our previous discussion of the BADOM and BDOM formulations (see also Harvey 1986).

The transient experiment given in Fig. 7 defines our standard experiment. This figure gives the time-dependent responses of the surface air temperature (ΔT_a), the surface temperature (ΔT_s) and the deep-ocean mean temperature (ΔT_d). For this standard simulation, we have assumed a surface air temperature increase $\Delta T_{ae}(2 \times \text{CO}_2)$ equal to 3 K. In all our computations, as illustrated in Fig. 7, the surface air temperature warming is always larger than the surface temperature increase.

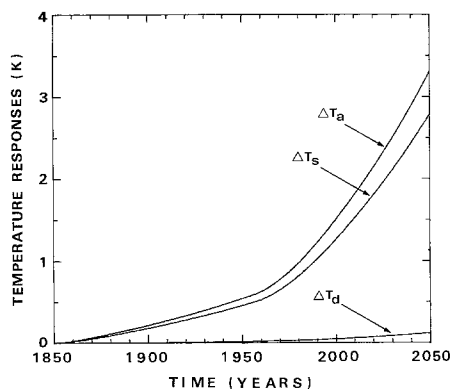


Fig. 7. Standard transient experiment with EBM-BADOM for a period between the pre-industrial time (1850) and the middle of the next century (2050). $\Delta T_{ae}(2 \times \text{CO}_2)$ is fixed at 3 K. ΔT_a , ΔT_s and ΔT_d are the surface air, the surface, and the vertically averaged deep ocean temperature responses, respectively

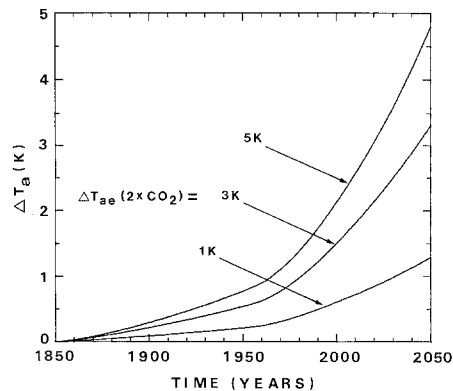


Fig. 8. Transient response for the surface air temperature (ΔT_a) obtained with EBM-BADOM for $\Delta T_{ae}(2 \times \text{CO}_2) = 1$ K, 3 K and 5 K

Furthermore, the difference between the two warmings increases slightly with time. This is related to the non-linear increase of latent-heat exchange between the surface and the atmosphere when the temperature increases, despite the decreasing difference between the surface air and surface temperatures.

To assess the model sensitivity to $\Delta T_{ae}(2 \times \text{CO}_2)$, Fig. 8 shows ΔT_a for three given values of $\Delta T_{ae}(2 \times \text{CO}_2)$ (1 K, 3 K and 5 K). As discussed already, this range of uncertainty is representative of equilibrium CO_2 climate experiments. The transient response ranges between 0.4 and 1.4 K in 1980, between 0.7 and 2.6 K in 2010, and between 1.3 and 4.8 K in 2050. By comparison with the equivalent equilibrium computations described earlier (see Fig. 5), these transient responses indicate that the oceanic heat uptake reduces the model response by around 10% for $\Delta T_{ae}(2 \times \text{CO}_2) = 1$ K, 25% for $\Delta T_{ae}(2 \times \text{CO}_2) = 3$ K, and 35% for $\Delta T_{ae}(2 \times \text{CO}_2) = 5$ K. More precisely, this reduction factor is shown to decrease slightly with time, varying for example from 27% in 1980 to 19% in 2050 for $\Delta T_{ae} = 3$ K, and shows a similar trend for other values of $\Delta T_{ae}(2 \times \text{CO}_2)$.

Equivalently, comparing Fig. 5 and Fig. 8 allows us to estimate the time delay for the global climate response from the instantaneous equilibrium response. Furthermore, Fig. 9 allows another estimation of the role of the oceanic heat capacity by giving the time-dependent response of the equilibrium global temperature (ΔT_e), the surface air temperature, if the heat exchange between the mixed layer and the deeper ocean is neglected and if the standard ΔT_a is obtained by the complete model. The importance of the deeper oceanic heat uptake is clearly illustrated by this figure; while at the same time the mixed layer is

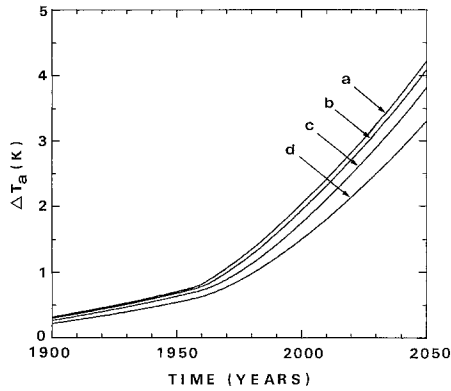


Fig. 9. Sensitivity to modelling the coupling of the ocean to the atmosphere. *Curve a* gives the time evolution of the instantaneous equilibrium surface temperature for the radiative perturbation shown in Fig. 4 (effective CO_2), using Eq. (1). *Curve b* gives the transient response of the surface air temperature for EBM coupled to a single oceanic mixed layer with a depth of 30 m. *Curve c* is similar to *curve b* but with an oceanic mixed-layer depth of 100 m. *Curve d* gives the standard transient experiment obtained with EBM-BADOM. All computations assume $\Delta T_{ac}(2 \times \text{CO}_2) = 3 \text{ K}$

shown to introduce by itself only a small time delay on the equilibrium response, rather independently of the precise value of the mixed-layer depth.

To test the model response to the BADOM formulation, we made a few sensitivity studies by changing, arbitrarily by a factor two, the values of the diffusion coefficient, K , and of the upwelling velocity, W . Figure 10 summarizes these sensitivity experiments. *Curve c* is the standard simulation with standard K and W values. *Curves b* and

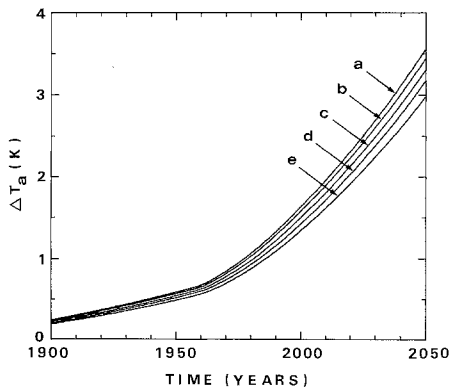


Fig. 10. Sensitivity experiments on the values of parameters K and W in the BADOM formulation. *Curve a* for the EBM-BADOM experiment with $K = 0.3 \text{ cm}^2 \text{ s}^{-1}$ and $W = 4 \text{ m year}^{-1}$; *curve b* for $K = 0.3 \text{ cm}^2 \text{ s}^{-1}$ and $W = 2 \text{ m year}^{-1}$; *curve c* for the standard EBM-BADOM experiment with $K = 0.6 \text{ cm}^2 \text{ s}^{-1}$ and $W = 4 \text{ m year}^{-1}$; *curve d* for $K = 1.2 \text{ cm}^2 \text{ s}^{-1}$ and $W = 8 \text{ m year}^{-1}$; *curve e* for $K = 1.2 \text{ cm}^2 \text{ s}^{-1}$ and $W = 4 \text{ m year}^{-1}$

d have been obtained by varying K and W simultaneously so as to keep the scale depth K/W constant, such that the observed deep ocean temperature profile is correctly simulated (as in the standard experiment). *Curves a* and *e* have been obtained without maintaining constant scale depth, and the ocean temperature profile degrades in comparison with data. If we disregard these last two simulations, the other three show that the model is rather insensitive to the accuracy of the K and W values. If the upwelling velocity W is suppressed, a purely diffusive formulation for the heat exchange into the ocean (BDOM formulation, defined earlier) is obtained. For such a BDOM formulation, similar sensitivity experiments were made with the value of the diffusion coefficient K (Fig. 11, K varying between 0.6 and $5 \text{ cm}^2 \text{ s}^{-1}$). In comparison to the results given in Fig. 10, the model response here appears to be more sensitive to the adopted K value. Harvey (1986) has already mentioned these different model behaviours for the BADOM and BDOM formulations by comparing model responses for an instantaneous CO_2 doubling. He concluded that, because of our ignorance of the exact K (and W) value to use in globally averaged models, the BADOM formulation should be preferred to the BDOM formulation. In Fig. 11, *curve a* gives the standard BADOM experiment. For the values of the oceanic parameters used here, the comparison of this BADOM simulation with the three BDOM simulations illustrates the faster response of the BADOM formulation, as already mentioned in the previous section.

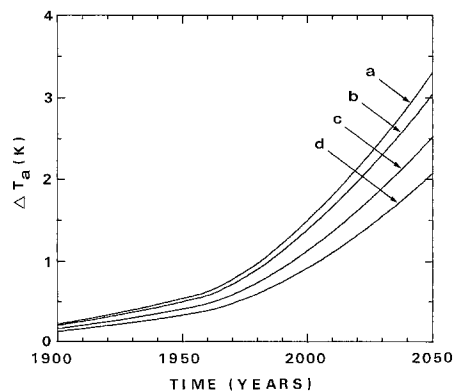


Fig. 11. Sensitivity experiments on the value of parameter K in the BDOM formulation. The mixed-layer depth is fixed to 30 m as in all BADOM experiments. *Curve a* gives the standard transient EBM-BADOM experiment for comparison. The three other curves are obtained using the BDOM formulation; *curve b* is for $K = 0.6 \text{ cm}^2 \text{ s}^{-1}$; *curve c* for $K = 2 \text{ cm}^2 \text{ s}^{-1}$; and *curve d* for $K = 5 \text{ cm}^2 \text{ s}^{-1}$

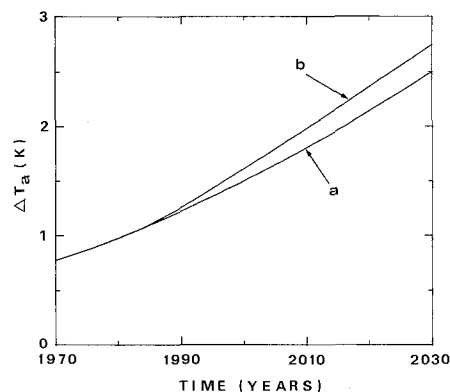
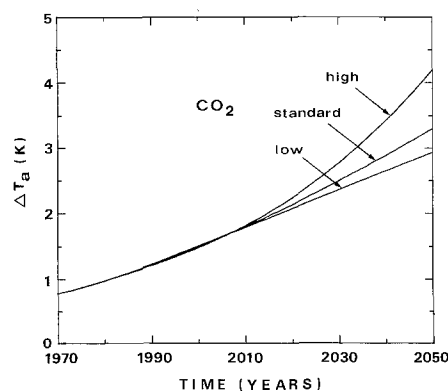
Table 7. Radiative perturbations at the tropopause (ΔQ_T) for variations in trace gas concentration. These values have been estimated with Eq. (1) and Table 6 of Ramanathan et al. (1985) using $\lambda = 1.92 \text{ Wm}^{-2} \text{ K}^{-1}$

Trace gas	Initial mixing ratio (ppbv)	Final mixing ratio (ppbv)	ΔQ_T (Wm^{-2})
CH ₄	1650	3300	0.60
N ₂ O	300	600	0.77
CFCl ₃	0	1	0.27
CF ₂ Cl ₂	0	1	0.31
CF ₂ HCl	0	1	0.09
CH ₃ CCl ₃	0	1	0.04
CCl ₄	0	1	0.15

Our standard scenarios for future trace gas concentrations are only thought to give a reasonable extrapolation of present trace gas trends, without taking future new energy policy into account. Therefore, we have undertaken two experiments to estimate the importance of the adopted future scenarios on the model response. In Fig. 12, we compare our standard ΔT_a with that obtained by modifying only our future scenarios to reach the trace gas concentrations adopted by Ramanathan et al. (1985) in the year 2030. We have already compared the difference of the equilibrium temperature responses for the 1980–2030 period using our standard scenarios and those of Ramanathan et al. (Let us recall that in Table 3 the equilibrium model response was fixed at 1.9 K for a CO₂ doubling.) In the transient case, Fig. 12 shows that the difference in the model response amounts to 0.25 K in 2030, the largest temperature response again being obtained with the scenarios of Ramanathan et al. Indeed, the oceanic

heat uptake introduces a time lag in the model response but does not change the relative importance of each trace gas. Therefore, our discussion concerning the difference of the relative importance for CH₄ and equivalent CFC in both scenarios remains qualitatively valid for the transient case.

However, the most significant climatic uncertainty for the near future is related to the future estimated CO₂ concentration. As an illustration, Fig. 13 gives the future ΔT_a for the three CO₂ scenarios proposed by Wuebbles et al. (1984), referred to as high, standard and low CO₂ scenarios. The range of temperature warming is around 1.8 K in 2010 and between 2.9 and 4.2 K in 2050. Clearly, our ignorance of the exact future CO₂ concentration levels is alone sufficient to prevent us from making a precise quantitative prediction of the climatic change in the next century, even if the models used simulated in a reliable way the behaviour of the climate system on the human time scale.

**Fig. 12.** Surface air transient response over the period 1970–2030 for the standard scenarios (curve *a*) and adopting the trace gas concentrations given by Ramanathan et al. (1985) for 2030 (curve *b*). These results have been obtained with EBM-BADOM**Fig. 13.** Surface air transient response (ΔT_a) for the three scenarios of the future CO₂ concentrations given in Fig. 2a. These results have been obtained with EBM-BADOM

Finally, it is worth noting that all our previous experiments were undertaken assuming a pre-industrial CO_2 concentration equal to 270 ppmv. But, as mentioned earlier, the pre-industrial CO_2 concentration level is only known approximately. Reliable knowledge of this model parameter is, however, very important for testing the skill of climate models by comparing the model results with the observational temperature trends since pre-industrial times. To illustrate the effect of such uncertainty on our model response, Fig. 14a and b gives the computed ΔT_a between 1850 and 1980 as a function of the equilibrium surface air temperature increase for a doubled CO_2 concentration, $\Delta T_{ae}(2 \times \text{CO}_2)$. The results are shown for five values of the assumed pre-industrial CO_2 concentration. In Fig. 14b, the climatic effect of the other trace gases is included in the computations following our standard trace gas scenarios. This figure illustrates the importance of the equilibrium model response to a CO_2 doubling for a quantitative estimate of climatic changes. But the computed past warming is also shown to be sensitive to the adopted pre-industrial CO_2 concentration. For example, Fig. 14b shows that for $\Delta T_{ae}(2 \times \text{CO}_2)$ equal to 3 K, the computed warming amounts to between 0.7 and 1.0 K for a pre-industrial CO_2 concentration between 290 and 270 ppmv. Similarly, for lower $\Delta T_{ae}(2 \times \text{CO}_2) = 1$ K, the warming ranges between 0.3 and 0.4 K and, for higher $\Delta T_{ae}(2 \times \text{CO}_2) = 5$ K, between 1.0 and 1.4 K.

The land surface air temperature trend is probably the most reliable and well-established temperature trend over the past 100 years and different northern-hemisphere land-based studies give essentially similar results, i.e. a warming to around 1940, a slight cooling to the mid-1960s and a warming since around 1970 (Wigley et al. 1985; Goossens and Berger 1986). However, recent studies allow us to begin reconstructing the recent past trends of three temperature series: surface air temperatures over oceans, surface air temperatures over land and sea surface temperatures (Chen 1982; Folland et al. 1984; Folland and Kates 1984; Barnett 1985). Whether these three sets of trends (especially for sea surface temperature and atmospheric temperatures) are in phase or display lags between them in the previous 100 years is not yet very clear because of the uncertainties in the various data sets due to the many problems in obtaining homogeneous time series of ship-based data (e.g., Folland et al. 1984), and in urban warming (Kukla et al. 1986). Averaged observational data indicate a global warming of

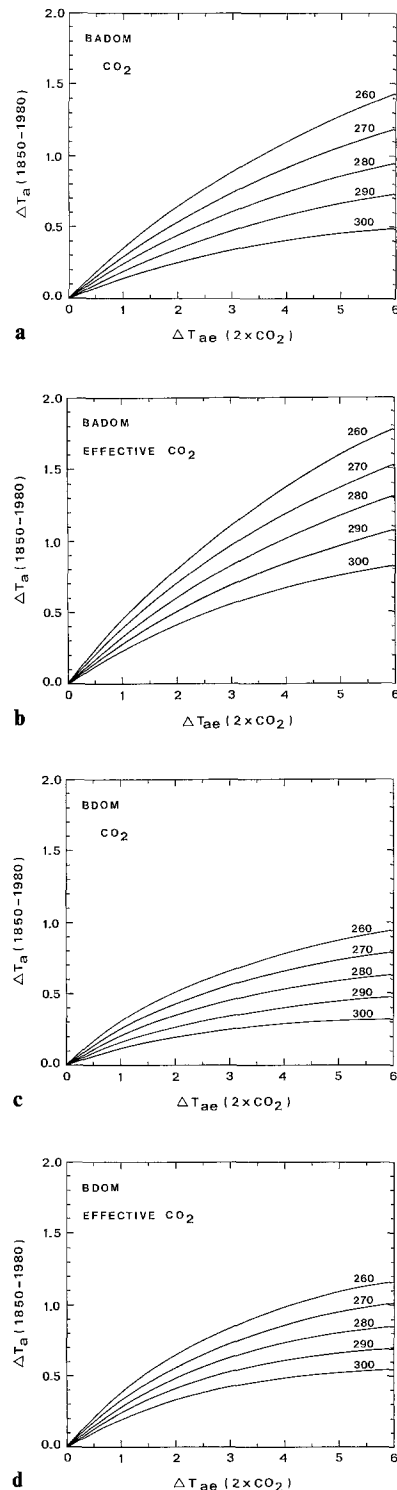


Fig. 14a–d. Surface air temperature increase between the pre-industrial time (1850) and the present (1980). The results are given as a function of $\Delta T_{ae}(2 \times \text{CO}_2)$ ranging from 0 to 6 K and of the pre-industrial CO_2 concentration ranging from 260 to 300 ppmv: **a** using our standard EBM-BADOM but for CO_2 alone; **b** as in **a**, but for the effective (or equivalent) CO_2 concentration (see Fig. 3); **c** using an EBM-BDOM with $K = 2 \text{ cm}^2 \text{ s}^{-1}$, for CO_2 alone; **d** as in **c**, but for the effective CO_2 concentration

about 0.5 K (between 0.3 and 0.7 K) since the late nineteenth century (Folland and Kates 1984; Wigley et al. 1985; UNEP-WMO-ICSU 1985; Jones et al. 1986). Figure 14b shows that the model results apparently agree with these observational trends for low values of $\Delta T_{ae}(2 \times \text{CO}_2)$. On the other hand, considering only CO_2 variation, Schlesinger (1986) indicates that the BDOM formulation can also give results that do not conflict with the observational record if a higher value of $\Delta T_{ae}(2 \times \text{CO}_2)$ (4 K) is combined with an effective diffusion coefficient K around $2 \text{ cm}^2 \text{ s}^{-1}$.

In order to test the sensitivity to the advective part of the ocean model and compare our results with those of Schlesinger, we performed sensitivity experiments similar to Fig. 14b (where BADOM was used) but for BDOM formulation and with $K=2 \text{ cm}^2 \text{ s}^{-1}$. Considering only CO_2 variation (Fig. 14c), a surface air warming of around 0.7 K, similar to that obtained by Schlesinger (1986), is found for $\Delta T_{ae}(2 \times \text{CO}_2)=4 \text{ K}$ and a pre-industrial CO_2 concentration of 270 ppmv. The inclusion of the other trace gases leads to a surface air warming of around 0.9 K for the same fixed parameters (Fig. 14d). Simultaneously, a warming of 0.5 K is found for a $\Delta T_{ae}(2 \times \text{CO}_2)$ which is taken as either 1.7 K or 2.6 K, according to a pre-industrial CO_2 concentration of either 270 ppmv or 290 ppmv. This means that the introduction of advection in the ocean model lowers the $\Delta T_{ae}(2 \times \text{CO}_2)$ value needed to account for a 0.5 K increase of surface air temperature between 1850 and 1980. This is in agreement with our conclusion comparing BDOM and BADOM impacts on the time lag induced by the deeper ocean inertia. (The time lag is shorter with BADOM formulation than with BDOM formulation, as shown in the previous section and Fig. 11.)

However, the similarity of data with computations does not validate any of the models in a definitive way because of the numerous assumptions included in these models as reviewed above. Moreover, it must also be stressed that, in the above experiments, only forcing induced by CO_2 and a few other trace gases has been included, neglecting other possible forcings on the decadal time scale such as volcanism, solar luminosity and solar activity. Much effort must now be devoted to the model validation with observational data.

Conclusions

To assess the climatic change caused by the variations of the trace gas concentrations in the past

and in the near future, current simple and sophisticated models can provide us with semi-quantitative, and sometimes only qualitative, results because of numerous uncertainties in the present climate models.

Major possible physical deficiencies of the climate models concern the parameterization of the main components of the hydrological cycle (mainly cloudiness and soil moisture), of the oceanic horizontal heat transport, of the sea-ice extent, and of the heat exchange between the upper and lower oceanic layers. The development of coupled atmosphere — ocean — cryosphere models and extensive and continuous measurements of the parameters of the climate system are indispensable for a full understanding of the global climate and ultimately for a more reliable prediction of transient climatic changes in the near future.

Moreover, future scenarios for the trace gas concentrations are only indicative, depending on future energy use. Even past trace gas concentrations are only known approximately. Keeping these uncertainties in mind, we have estimated a possible range for the global temperature change from the pre-industrial epoch to the middle of the next century using a simple global climate model. Using the past and future scenarios given by Wuebbles et al. (1984), a model response — equal to 3 K — to a CO_2 doubling and an advective-diffusive parameterization for the oceanic heat uptake, our standard experiment gives a total surface air warming of 1.0 K due to the probable change in the concentration of the trace gases between the pre-industrial period and the present. The CO_2 -induced warming alone amounts to 0.75 K, i.e. 75% of the total warming. For a pre-industrial CO_2 concentration of 290 ppmv, the warming is 0.77 K and the CO_2 -induced warming amounts to 0.50 K, i.e. 65% of the total warming. Over the next 70 years, our standard experiment gives a possible global mean surface air warming of 2.3 K with the CO_2 contribution amounting to 1.6 K, i.e., 70% of the total warming. Because of the simplified radiative scheme used in our computations, these relative contributions for CO_2 alone can be overestimated by roughly 15%.

To take the present uncertainties in the climate sensitivity to trace gas changes into account, an assumed increase in the equilibrium temperature of between 1 K and 5 K seems reasonable for a CO_2 doubling. For such a range of equilibrium temperature increase, the global mean surface air warming between 1850 and the present is estimated to range between 0.4 and 1.4 K for a pre-

industrial CO₂ concentration equal to 270 ppmv. A pre-industrial CO₂ concentration of 290 ppmv lowers the range to between 0.3 and 1 K. For the same range of equilibrium temperature increase, the surface air warming is estimated to amount to between 0.9 and 3.4 K over the next 70 years, for the standard trace gas scenarios of Wuebbles et al. (1984).

Although the majority of involved scientists agree that the problem of a possibly changing climate due to the emission of greenhouse gases should be considered as one of today's most important long-term environmental problems (Executive Summary, UNEP-WMO-ICSU, 1985), a better quantitative estimate of the climatic change (especially precipitation and regional changes) due to these increasing trace gas concentrations is needed to provide a rational basis to policy makers.

Appendix

To estimate the total trace-gas-induced radiative perturbation at the tropopause, we develop the total perturbation ΔQ_T as follows (Wigley 1985):

$$\Delta Q_T(t) = \Delta Q_{\text{CO}_2}(t) + \Delta Q_{\text{CH}_4}(t) + \Delta Q_{\text{N}_2\text{O}}(t) + \sum_i \Delta Q_{\text{CFC}_i}(t). \quad (19)$$

For CH₄ and N₂O, ΔQ is estimated to be proportional to the square-root of concentration, i. e.

$$\Delta Q_{\text{CH}_4}(t) = a_1 (\sqrt{C[\text{CH}_4]_t} - \sqrt{C[\text{CH}_4]_{t_0}}) \quad (20)$$

$$\Delta Q_{\text{N}_2\text{O}}(t) = a_2 (\sqrt{C[\text{N}_2\text{O}]_t} - \sqrt{C[\text{N}_2\text{O}]_{t_0}}) \quad (21)$$

with $C[\text{CH}_4]_t$ and $C[\text{N}_2\text{O}]_t$ the actual trace gas concentrations at time t , and $C[\text{CH}_4]_{t_0}$ and $C[\text{N}_2\text{O}]_{t_0}$ the initial trace gas concentrations; whereas for chlorocarbons we assume a linear relationship with concentration, i. e.

$$\Delta Q_{\text{CFC}_i}(t) = a_{3i} (C[\text{CFC}_i]_t - C[\text{CFC}_i]_{t_0}). \quad (22)$$

We can combine the effects of various [CFC]_{*i*} by defining a radiatively weighted mean concentration $C[\text{CFC}]$ as

$$\begin{aligned} \Delta Q_{\text{CFC}}(t) &= \sum_{i=1}^n \Delta C_{[\text{CFC}_i]_t}(t) \\ &= \sum_{i=1}^n a_{3i} \Delta C[\text{CFC}_i] \end{aligned}$$

$$\begin{aligned} &= a_3 \sum_{i=1}^n \frac{a_{3i}}{a_3} \Delta C[\text{CFC}_i] \\ &= a_3 \Delta C[\text{CFC}]_t \\ &\quad (\text{or } a_3 C[\text{CFC}]_t \text{ if } t_0 = 1850) \quad (23) \end{aligned}$$

where $\Delta C[\text{CFC}]_t$ is the radiatively weighted mean chlorocarbons concentration variation.

From Ramanathan et al. (1985), Table 7 is obtained which gives

$$\begin{aligned} a_1 &= 0.035 \\ a_2 &= 0.107 \\ a_3 &= 0.308. \end{aligned}$$

With this value of a_3 , $\Delta C[\text{CFC}]_t$ introduced in Eq. (23) can be developed as in Eq. (5).

Finally, we obtain the following equation from Eq. (19) with Eqs. (6), (20), (21) and (23) (for $t_0 = 1850$):

$$\begin{aligned} \Delta Q_T(t) &= \Delta Q_{\text{CO}_2}(2 \times) \\ &\quad \times \ln(\tilde{C}[\text{CO}_2]_t / C[\text{CO}_2]_{t_0}) / \ln 2 \end{aligned} \quad (24)$$

with the effective CO₂ concentration, $\tilde{C}[\text{CO}_2]$, defined by

$$\begin{aligned} \tilde{C}[\text{CO}_2]_t &= C[\text{CO}_2]_t \\ &\quad \times \exp\{0.00599 \\ &\quad (\sqrt{C[\text{CH}_4]_t} - \sqrt{C[\text{CH}_4]_{t_0}}) \\ &\quad + 0.01812 (\sqrt{C[\text{N}_2\text{O}]_t} - \sqrt{C[\text{N}_2\text{O}]_{t_0}}) \\ &\quad + 0.05139 (C[\text{CFC}]_t)\} \end{aligned} \quad (25)$$

Eq. (25) defines a CO₂ concentration which is as radiatively effective as would be the combined concentrations of CO₂ and other trace gases.

Acknowledgements. The authors wish to thank Prof. M. Schlesinger for stimulating discussions during his visit to the Institute of Astronomy and Geophysics G. Lemaître in Louvain-la-Neuve, and Dr. D. Harvey for providing us with an initial version of the atmospheric-oceanic energy balance model used in this study and for valuable comments and suggestions on a first draft of the present paper. We also thank one of the reviewers for language editing remarks. This work was supported in part by the Commission of the European Communities under contract CLI-076-B (RS).

References

- Ackerman TP (1979) On the effect of CO₂ on atmospheric heating rates. *Tellus* 31: 115–123
- Adem J, Garduno R (1984) Sensitivity studies on the climatic effect of an increase of atmospheric CO₂. *Geofis Int* 23(1): 17–37

- Augustsson T, Ramanathan V (1977) A radiative-convective model study of the CO₂ climate problem. *J Atmos Sci* 34: 448–451
- Barnett TP (1985) An long-term climate change in observed physical properties of the oceans. In: MacCracken MC, Luther FM (eds) *Detecting the climatic effects of increasing carbon dioxide*, DOE/ER-0235, US Department of Energy, Washington, DC, pp 91–107 Available from NTIS, Springfield, Virginia 22161
- Bohren CF (1985) Comment on “Cloud optical thickness. Feedbacks in the CO₂ climate problem”. *J Geophys Res* 90 (D3): 5867
- Bryan K, Spelman MJ (1985) The ocean’s response to a CO₂-induced warming. *J Geophys Res* 90(C6), 11: 679–688
- Bryan K, Komro FG, Rooth C (1984) The ocean’s transient response to global surface temperature anomalies. In: Hansen JE, Takahashi T (eds) *Climate processes and climate sensitivity*, Maurice Ewing series 5. American Geophysical Union, Washington DC, pp 29–38
- Centuno M (1982) New formulae for the equivalent night sky emissivity. *Solar Energy* 28(6): 489–498
- Cess RD (1985) Nuclear war: illustrative effects of atmospheric smoke and dust upon solar radiation. *Climatic Change* 7: 237–251
- Cess RD, Goldenberg SD (1981) The effect of ocean heat capacity upon the global warming due to increasing atmospheric carbon dioxide. *J Geophys Res* 86: 498–502
- Cess RD, Potter GL, Ghan SJ, Gates WL (1985) The climatic effects of large injections of atmospheric smoke and dust: a study of climate feedback mechanisms with one- and three-dimensional climate models. *J Geophys Res* 90(D7): 12,937–12,950
- Charlock TP (1981) Cloud optics as a possible stabilizing factor in climate change. *J Atmos Sci* 38: 661–663
- Charlock TP (1982) Cloud optical feedback and climate stability in a radiative-convective model. *Tellus* 34: 245–254
- Chen RS (1982) Combined land/sea surface air temperature trends, 1949–1972. Master’s Thesis, Department of Meteorology and Physical Oceanography, Massachusetts Institute of Technology, Cambridge
- Chou MD, Peng L, Arking A (1982) Climate studies with a multilayer energy balance model, Part II: the role of feedback mechanisms in the CO₂ problem. *J Atmos Sci* 39: 2657–2666
- Dickinson RE (1982) Modeling climate changes due to carbon dioxide increases. In: Clark WC (ed) *Carbon dioxide review*. Clarendon Press, pp 101–133
- Dickinson RE (1985) How will climate change? In: UNEP-WMO-ICSU report on the assessment of the role of carbon dioxide and of other greenhouse gases in climate variations and associated impacts. Wiley (in press)
- Flohn H (1978) Estimates of a combined greenhouse effect as background for a climate scenario during global warming. In: Williams J (ed) *Carbon dioxide, climate and society*. IIASA Proceedings series, Environment, Pergamon, Oxford, pp 227–237
- Folland CK, Kates FE (1984) Changes in decadal averaged sea surface temperature over the world 1861–1980. In: Berger A et al. (eds) *Milankovitch and climate*, part 2. Reidel, Dordrecht, pp 721–727
- Folland CK, Parker DE, Kates FE (1984) Worldwide marine temperature fluctuations, 1856–1981. *Nature* 310: 670–673
- Garrett C (1979) Mixing in the ocean interior. *Dyn Atmos Oceans* 3: 239–265
- Gates WL (1981) The climate system and its portrayal by climate models: a review of basic principles. II: Modeling of climatic changes. In: Berger A (ed) *Climatic variations and variability: facts and theories*. Reidel, Dordrecht, pp 435–459
- Gates WL, Cook KH, Schlesinger ME (1981) Preliminary analysis of experiments on the climatic effects of increased CO₂ with an atmospheric general circulation model and a climatological ocean. *J Geophys Res* 86: 6385–6393
- Gilchrist A (1983) Increased carbon dioxide concentrations and climate: the equilibrium response. In: Bach W et al. (eds) *Carbon dioxide: current views and developments in energy/climate research*. Reidel, Dordrecht, pp 219–258
- Goossens Chr, Berger A (1986) Annual and seasonal climatic variations over the Northern Hemisphere and Europe during the last century. *Ann Geophys* 48: 385–400
- Gutowski WJ, Wang WC, Stone PH (1985) Effects of dynamic heat fluxes on model climate sensitivity: meridional sensible and latent heat fluxes. *J Geophys Res* 90(D7): 13,081–13,086
- Hansen J, Johnson D, Lacis A, Lebedeff S, Lee P, Rind D, Russell G (1981) Climate impact of increasing atmospheric carbon dioxide. *Science* 213: 957–966
- Hansen J, Lacis A, Rind D, Russell G, Stone P, Fung I, Ruedy R, Lerner J (1984) Climate sensitivity: analysis of feedback mechanisms. In: Hansen JE, Takahashi T (eds) *Climate processes and climate sensitivity*, Maurice Ewing series 5. American Geophysical Union, Washington DC, pp 130–163
- Harvey LD (1986) Effect of ocean mixing on the transient climate response to a CO₂ increase: analysis of recent model results. *J Geophys Res* 91(D2): 2709–2718
- Harvey LD, Schneider SH (1985a) Transient climate response to external forcing on 10⁰–10⁴ year time scales. Part 1: Experiments with globally averaged, coupled, atmosphere and ocean energy balance models. *J Geophys Res* 90(D1): 2191–2205
- Harvey LD, Schneider SH (1985b) Transient climate response to external forcing on 10⁰–10⁴ year time scales. Part 2: Sensitivity experiments with a seasonal, hemispherically averaged, coupled atmosphere, land, and ocean energy balance model. *J Geophys Res* 90(D1): 2207–2222
- Heintzenberg J, Ogren JA (1985) An assessment of the impact of pollution on global cloud albedo: comment. *Tellus* 37B: 308–309
- Hibler WD III (1984) The role of sea-ice dynamics in modeling CO₂ increases. In: Hansen JE, Takahashi T (eds) *Climate processes and climate sensitivity*. Geophys Monogr n°29, Maurice Ewing Series 5, American Geophysical Union, Washington DC, pp 238–253
- Hoffert MI, Flannery BP (1985) Model projections of the time-dependent response to increasing carbon dioxide. In: MacCracken MC, Luther FM (eds) *The potential climatic effects of increasing carbon dioxide*. DOE/ER-0237 US Department of Energy, Washington DC, pp 149–190
- Hoffert MI, Callegari AJ, Hsieh C-T (1980) The role of deep sea storage in the secular response to climate forcing. *J Geophys Res* 85(C11): 6667–6679
- Hummel JR (1982a) Surface temperature sensitivities in a multiple cloud radiative-convective model with a constant and pressure dependent lapse rate. *Tellus* 34: 203–208
- Hummel JR (1982b) Anomalous water-vapor absorption: implications for radiative-convective models. *J Atmos Sci* 39: 879–885
- Hummel JR, Kuhn WR (1981a) Comparison of radiative-convective models with constant and pressure-dependent lapse rates. *Tellus* 33: 254–261

- Hummel JR, Kuhn WR (1981b) An atmospheric radiative-convective model with interactive water vapor transport and cloud development. *Tellus* 33: 372–381
- Hummel JR, Reck RA (1981) Carbon dioxide and climate: the effects of water transport in radiative-convective models. *J Geophys Res* 86(C12): 12,035–12,038
- Hunt BG (1981) An examination of some feedback mechanisms in the carbon dioxide climate problem. *Tellus* 33: 78–88
- Hunt BG, Wells NC (1979) An assessment of the possible future climate impact of carbon dioxide increases based on a coupled one-dimensional atmospheric-oceanic model. *J Geophys Res* 84: 787–791
- Idso SB (1980) The climatological significance of a doubling of earth's atmospheric carbon dioxide concentration. *Science* 207: 1462–1463
- Jones PD, Wigley TML, Wright PB (1986) Global temperature variations between 1861 and 1984. *Nature* 322 (6078): 430–434
- Kandel RS (1981) Surface temperature sensitivity to increased atmospheric CO₂. *Nature* 293: 634–636
- Kiehl JT, Ramanathan V (1982) Radiative heating due to increased CO₂: the role of H₂O continuum absorption in the 12–18 μm region. *J Atmos Sci* 39: 2923–2926
- Kukla G, Gavin J, Karl TR (1986) Urban warming. *J Climate Appl Meteorol* 25: 1265–1270
- Lal M, Ramanathan V (1984) The effects of moist convection and water vapor radiative processes on climate sensitivity. *J Atmos Sci* 41: 2238–2249
- Lal M, Dube SK, Sinha PC, Jain AK (1986) Potential climatic consequences of increasing anthropogenic constituents in the atmosphere. *Atmos Environ* 20(4): 639–642
- Li Y-H, Peng T-H, Broecker WS, Ostlund HG (1984) The average vertical mixing coefficient for the oceanic thermocline. *Tellus*, 36B: 212–217
- Lindzen RS, Hou AY, Farrell BF (1982) The role of convective model choice in calculating the climate impact of doubling CO₂. *J Atmos Sci* 39: 1189–1205
- Luther FM, Cess RD (1985) Review of the recent carbon dioxide-climate controversy. In: MacCracken MC, Luther FM (eds) *The potential climatic effects of increasing carbon dioxide*. DOE/ER-0237, US Department of Energy, Washington, pp 323–335
- Manabe S (1971) Estimate of future changes in climate due to increase of carbon dioxide concentration in the air. In: Mathews WH, Kellogg WW, Robinson GD (eds) *Man's impact on the climate*, MIT Press, Cambridge, Massachusetts, pp 249–264
- Manabe S (1983) Carbon dioxide and climatic change. *Adv Geophys* 25: 39–82
- Manabe S, Stouffer RJ (1980) Sensitivity of a global climate model to an increase of CO₂ concentration in the atmosphere. *J Geophys Res* 85: 5529–5554
- Manabe S, Wetherald RT (1967) Thermal equilibrium of the atmosphere with a given distribution of relative humidity. *J Atmos Sci* 24: 241–259
- Manabe S, Wetherald RT (1975) The effect of doubling the CO₂ concentration on the climate of a general circulation model. *J Atmos Sci* 32(1): 3–15
- Manabe S, Wetherald RT (1980) On the distribution of climate change resulting from an increase in CO₂-content of the atmosphere. *J Atmos Sci* 37: 99–118
- Moller F (1963) On the influence of changes in CO₂ concentration in air on the radiative balance of the earth's surface and on the climate. *J Geophys Res* 68: 3877–3886
- Neftel A, Moor E, Oeschger H, Stouffer B (1985) Evidence from polar ice cores for the increase in atmospheric CO₂ in the past two centuries. *Nature* 315: 45–47
- Newell RE, Dopplick TG (1979) Questions concerning the possible influence of anthropogenic CO₂ on atmospheric temperature. *J Appl Meteorol* 18: 822–825
- North GR, Mengel JG, Short DA (1984) On the transient response patterns of climate to time-dependent concentrations of atmospheric CO₂. In: Hansen JE, Takahashi T (eds) *Climate processes and climate sensitivity*, Maurice Ewing Series 5, American Geophysical Union, Washington DC, pp 164–170
- Ohring G, Adler S (1978) Some experiments with a zonally averaged climate model. *J Atmos Sci* 35: 186–205
- Ou SCS, Liou KN (1984) A two-dimensional radiation-turbulence climate model. 1. Sensitivity to cirrus radiative properties. *J Atmos Sci* 41: 2289–2309
- Ou SCS, Liou KN (1985) Cumulus convection and climatic temperature perturbations. *J Geophys Res* 90(D1): 2223–2232
- Potter GL (1980) Zonal model calculation of the climatic effect of increased CO₂. In: Singh JJ, Deepak A (eds) *Environmental and climatic impact of coal utilization*, Academic Press, New York, pp 433–454
- Ramanathan V (1981) The role of ocean-atmosphere interactions in the CO₂ climate problem. *J Atmos Sci* 38: 918–930
- Ramanathan V, Lian MS, Cess RD (1979) Increased atmospheric CO₂: zonal and seasonal estimates of the effect on the radiation energy balance and surface temperature. *J Geophys Res* 84: 4949–4958
- Ramanathan V, Cicerone RJ, Singh HB, Kiehl JT (1985) Trace gas trends and their potential role in climate change. *J Geophys Res* 90(D3): 5547–5566
- Rasool SI, Schneider SH (1971) Atmospheric carbon dioxide and aerosols: effects of large increases on global climate. *Science* 173: 138–141
- Raynaud D, Barnola JM (1985) An Antarctic ice core reveals atmospheric CO₂ variations over the past few centuries. *Nature* 315: 309–311
- Rowntree PR, Walker J (1978) The effects of doubling the CO₂ concentration on radiative-convective equilibrium. In: Williams J (ed) *Carbon dioxide, climate and society*, Pergamon, Oxford, pp 181–191
- Schlesinger ME (1983) A review of climate model simulations of CO₂-induced climatic change. Report N°41, Climatic Research Institute, Oregon State University, Corvallis
- Schlesinger ME (1984) Climate model simulation of CO₂-induced climatic change. *Adv Geophys* 26: 141–235
- Schlesinger ME (1985) Analysis of results from energy balance and radiative-convective models. In: MacCracken MC, Luther FM (eds) *The potential climatic effects of increasing carbon dioxide*. DOE/ER-0237, US Department of Energy, Washington DC, pp 281–319
- Schlesinger ME (1986) Equilibrium and transient climatic warming induced by increased atmospheric CO₂. *Climate Dynamics* 1: 35–51
- Schlesinger ME, Mitchell JFB (1985) Model projections of the equilibrium climatic response to increased carbon dioxide. In: MacCracken MC, Luther FM (eds) *The potential climatic effects of increasing carbon dioxide*. DOE/ER-0237, US Department of Energy, Washington DC, pp 81–147
- Schlesinger ME, Gates WL, Han Y-J (1985) The role of the ocean in CO₂-induced climate change: preliminary results from the OSU coupled atmosphere-ocean general circula-

- tion model. In: Nihoul JCJ (ed) Coupled ocean-atmosphere models, Elsevier, pp 447–478
- Schneider SH, Dickinson RE (1974) Climate modeling. *Rev Geophys Space Phys* 12(3): 447–493
- Schneider SH, Thompson SL (1981) Atmospheric CO₂ and climate: importance of the transient response. *J Geophys Res* 86: 3135–3147
- Shine KP, Henderson-Sellers A (1983) Modelling climate and the nature of climate models: a review. *J Climatology* 3: 81–94
- Siegenthaler U (1983) Uptake of excess CO₂ by an outcrop-diffusion model of the ocean. *J Geophys Res* 88: 3599–3608
- Siegenthaler U, Oeschger H (1984) Transient temperature changes due to increasing CO₂ using simple models. *Ann of Glaciol* 5: 153–159
- Somerville RCJ, Remer LA (1984) Cloud optical thickness feedbacks in the CO₂ climate problem. *J Geophys Res* 89(D6): 9668–9672
- Temkin RL, Snell FM (1976) An annual zonally-averaged hemispherical climate model with diffuse cloudiness feedback. *J Atmos Sci* 33: 1671–1685
- Twomey SA, Piepgrass M, Wolfe TL (1984) An assessment of the impact of pollution on global cloud albedo. *Tellus* 36: 356–366
- UNEP-WMO-ICSU (1985) Report of the international conference on the assessment of the role of carbon dioxide and of other greenhouse gases in climate variations and associated impacts. WMO n°661
- Volz A (1983) Climatic impact of trace gases, aerosols, land-use changes and waste-heat release. In: Bach W et al. (eds) Carbon dioxide: current views and developments in energy/climate research, Reidel, Dordrecht, pp 353–378
- Wang WC, Molnar G (1985) A model study of the greenhouse effects due to increasing atmospheric CH₄, N₂O, CF₂Cl₂ and CFC₁₃. *J Geophys Res* 90: 12,971–12,980
- Wang WC, Ryan PB (1983) Overlapping effect of atmospheric H₂O, CO₂ and O₃ on the CO₂ radiative effect. *Tellus* 35B: 81–91
- Wang WC, Stone PH (1980) Effect of ice-albedo feedback on global sensitivity in a one-dimensional radiative-convective climate model. *J Atmos Sci* 37: 545–552
- Wang WC, Yung YL, Lacis AA, Mo T, Hansen JE (1976) Greenhouse effect due to man-made perturbations of trace gases. *Science* 194: 685–690
- Wang WC, Rossow WB, Yao MS, Wolfson M (1981) Climate sensitivity of a one-dimensional radiative-convective model with cloud feedback. *J Atmos Sci* 38(6): 1167–1178
- Wang WC, Molnar G, Mitchell TD, Stone PH (1984) Effects of dynamical heat fluxes on model climate sensitivity. *J Geophys Res* 89 (D3): 4699–4711
- Wang WC, Wuebbles DJ, Washington WM, Isaacs RG, Molnar G (1986) Trace gases and other potential perturbations to global climate. *Rev Geophys* 24(1): 110–140
- Washington WM, Meehl GA (1983) General circulation model experiments on the climatic effects due to a doubling and quadrupling of carbon dioxide concentration. *J Geophys Res* 88(11): 6600–6610
- Washington WM, Meehl GA (1984) Seasonal cycle experiment on the climate sensitivity due to a doubling of CO₂ with an atmospheric general circulation model coupled to a simple mixed-layer ocean model. *J Geophys Res* 89(D6): 9475–9503
- Watts RG (1985) Global climate variation due to fluctuations in the rate of deep water formation. *J Geophys Res* 90(D5): 8067–8070
- Weare BC, Snell FM (1974) A diffuse thin cloud structure as a feedback mechanism in global climatic modeling. *J Atmos Sci* 31: 1725–1734
- Wetherald RT, Manabe S (1986) An investigation of cloud cover change in response to thermal forcing. *Climatic Change* 8: 5–23
- Wigley TML (1985) Carbon dioxide, trace gases and global warming. *Climate Monitor* 13: 133–148
- Wigley TML, Jones PD (1981) Detecting CO₂-induced climatic change. *Nature* 292: 205–208
- Wigley TML, Schlesinger ME (1985) Analytical solution for the effect of increasing CO₂ on global mean temperature. *Nature* 315: 649–652
- Wigley TML, Angell JK and Jones PD (1985) Analysis of the temperature record. In: MacCracken MC, Luther FM (eds) Detecting the climatic effects of increasing carbon dioxide. DOE/ER-0235, US Department of Energy, Washington DC, pp 55–90. Available from NTIS, Springfield, Virginia 22161
- WMO (1982) The stratosphere 1981: theory and measurements. WMO Global Ozone Research and Monitoring Project, Report N°11
- WMO (1983 a) Report of the meeting of experts on potential climatic effects of ozone and other minor trace gases. Boulder, Colorado, 13–17 September 1982, WMO Global Ozone Research and Monitoring Project, Report N°14
- WMO (1983 b) Report of the WMO (CAS) meeting of experts on the CO₂ concentrations from pre-industrial times to I.G.Y. Boulder, Colorado, 22–25 June 1983, World Climate Programme, WCP-53, WMO/ICSU, Geneva, 34pp
- WMO (1986) Atmospheric ozone 1985. Assessment of our understanding of the processes controlling its present distribution and change. WMO Global Ozone Research and Monitoring Project, Report N°16, V.I, II and III
- Wuebbles DJ, MacCracken MC, Luther FM (1984) A proposed reference set of scenarios for radiatively active atmospheric constituents. US Department of Energy, Carbon Dioxide Research Division, Tech Rep 015

Received March 17, 1986/Accepted February 2, 1987